

MAY 10 1976

# Communications Research Centre

EXPERIMENTS WITH A MOBILE X-BAND FM RADAR  
IN MEASURING THE THICKNESS OF FRESH-WATER ICE

by

G.O. VENIER, F.R. CROSS AND R.O. RAMSEIER

IC



Department of  
Communications

Ministère des  
Communications

CRC TECHNICAL NOTE NO. 673

OTTAWA, OCTOBER 1975

LKC  
TK  
5102.5  
.R48e  
#673  
c.2

COMMUNICATIONS RESEARCH CENTRE

DEPARTMENT OF COMMUNICATIONS  
CANADA



EXPERIMENTS WITH A MOBILE X-BAND FM RADAR  
IN MEASURING THE THICKNESS OF FRESH-WATER ICE

by

G.O. Venier and F.R. Cross (CRC) and R.O. Ramseier (DOE)

*(Radio and Radar Branch)*  
*(Department of Environment)*



CRC TECHNICAL NOTE NO. 673

October 1975  
OTTAWA

**CAUTION**

This information is furnished with the express understanding that:  
Proprietary and patent rights will be protected.

100

100

100

100

100

TABLE OF CONTENTS

ABSTRACT . . . . . 1

1. INTRODUCTION . . . . . 1

2. DESCRIPTION OF RADAR . . . . . 2

3. RADAR PERFORMANCE IN THE LABORATORY . . . . . 3

    3.1 Radar Resolution . . . . . 3

    3.2 Water Attenuation Measurement . . . . . 4

    3.3 Comparison of Direct Radar and Tape Recorded Outputs . . . . . 5

    3.4 Comparison of Radar and Digital Recirculator Outputs . . . . . 5

4. FIELD TESTS . . . . . 5

    4.1 Radar Mounted on Sled . . . . . 5

    4.2 Radar Mounted on Air Cushion Vehicle (ACV) . . . . . 8

5. DOE ICE LABORATORY TESTS . . . . . 9

    5.1 Experimental Set-up . . . . . 9

    5.2 Experimental Results . . . . . 9

        5.2.1 Ice Growth . . . . . 9

        5.2.2 Water on Ice Surface . . . . . 10

        5.2.3 Snow on Ice Surface . . . . . 10

6. SUMMARY . . . . . 10

7. CONCLUSIONS . . . . . 12

8. ACKNOWLEDGEMENT . . . . . 12

9. REFERENCES . . . . . 13

EXPERIMENTS WITH A MOBILE X-BAND FM RADAR  
IN MEASURING THE THICKNESS OF FRESH-WATER ICE

by

G.O. Venier and F.R. Cross (CRC), and R.O. Ramseier (DOE)

ABSTRACT

The feasibility of using a high resolution FM radar at X-band frequencies, for measuring the thickness of fresh-water ice from a moving platform, was investigated in a series of field measurements during the winter of 1972/73. The radar was first mounted on a sled and towed over the ice by a snowmobile, and secondly, mounted on an air cushion vehicle and flown over the ice surface. The resolution capability of the radar was adequate for measuring a minimum ice thickness of 14 to 15 centimetres. Received signals were recorded on an audio magnetic tape recorder and processed in the laboratory using a digital computer as well as a slow sweep spectrum analyzer. Radar ice thickness measurements were also carried out during the summer months under controlled conditions in a DOE laboratory. The test results indicate that accurate ice thickness measurements can be carried out with a mobile X-band FM radar.

1. INTRODUCTION

During the winter of 1971/72, experiments were carried out on the snow and ice cover near Shirley Bay with an X-band FM radar that was developed at CRC. This work, originally a short term project, was carried out to determine the feasibility of measuring the depth of snow and the thickness of fresh-water

ice by means of radar. The results obtained from the brief series of tests indicated that radar waves were reflected from the surface of the snow and ice and from the snow-ground and ice-water interfaces respectively. These tests were described in an earlier CRC Technical Note [1].

As a result of these preliminary tests, the Radar Systems Engineering Section of CRC, in cooperation with the Floating Ice Section of the Department of the Environment, decided to continue the experiments. The tests were carried out during the winter of 1972/73 on (a) the St. Lawrence River between Wolfe Island and Kingston and (b) the Ottawa River. For the St. Lawrence River tests use was made of DOE's facilities at Wolfe Island. For the purpose of making measurements the radar was either mounted on a sled towed by a snow-mobile, or mounted on an air cushion vehicle (ACV).

Plans were also made to mount the radar on the deck of the MOT ice breaker "Griffin" for a cruise on Lake Erie during the period of maximum ice cover (February or March). Unfortunately, the ice cover on Lake Erie was so sparse throughout the winter of 1972/73 that these tests were cancelled.

Arrangements are being made to mount a more compact and improved version of the radar on an MOT Prescott-based helicopter. During the winter of 1973/74 the radar will be flown over the ice cover on the St. Lawrence River to measure the thickness of ice in the Seaway.

## 2. DESCRIPTION OF RADAR

The theory of operation of the radar was described in Ref. 1. For the tests described in this report several modifications were made to the system to improve its performance. The original travelling wave tube (TWT) amplifier was replaced with a 10 watt TWT, the coaxial circulator was replaced with a waveguide type, and solid state video amplifiers and filter units replaced the tube models previously used. A Uher (Model 4000) tape recorder was added to the original system to provide a means of data storage; also, a digital recirculating unit, developed at CRC, was added to provide a capability for obtaining an instantaneous record or "snapshot" from a single point while the radar was in motion. Figure 1 shows a block diagram of the system.

A block diagram of the digital recirculator is shown in Figure 2. A 64 millisecond record, consisting of up to 256 digitized samples of the detected video signal, is captured in a shift register 256 bits long by eight bits wide. This record is then recirculated through the shift register for a time long enough to allow the low speed spectrum analyzer to plot the spectrum. Thus, a plot of the radar return versus range, at the instant the recirculator is manually commanded to sample, is produced within the following minute. Radar operation, and the analog video recording described above, can thus proceed in parallel with the low-speed processing of a single record.

A photograph of the radar is shown in Figure 3. The sweep generator is in the bottom compartment with the TWT immediately above it in the second compartment. The third compartment contains the digital recirculator on the left and the pen recorder on the right. The wave analyzer is shown in the fourth compartment. The top compartment contains the tape recorder on the

left and a frequency counter on the right. The horn antenna is connected directly to the waveguide circulator while the RF filter, (connected to Port 3 of the circulator), and the detector are mounted inside the metal box at the end of the antenna boom.

### 3. RADAR PERFORMANCE IN THE LABORATORY

#### 3.1 RADAR RESOLUTION

The resolution of the radar was measured on a radar range, which was nine feet (2.7m) in length, four feet (1.2m) in height and three feet (0.9m) in width. A photograph of the range is shown in Figure 4. The range, constructed of radar absorbent material, effectively eliminated the transmission of unwanted radiation and concomitant reflections. Figure 5 shows the spectrum obtained when there was no target in the range. The small return signal shown was caused by a metal panel behind the rear wall of the range. The range resolution of the radar was measured by mounting two flat metal plates, six inches (15.2 cm) square, in the range, one fixed and one moveable, and measuring the separation between the plates first by radar and then by conventional means.

Figure 6 shows the results obtained for two oscillator sweep rates when the plates were 10 inches (25.4 cm) apart. The curves of Figures 6a and 6b were obtained using respectively oscillator sweep durations of 400 msec and 150 msec, the former corresponding to that reported in Ref. 1. It is evident from Figure 6 that the higher sweep rate (duration of 150 milliseconds) produced a smoother curve that was easier to interpret than that produced with the 400 millisecond sweep. The change in sweep rate, with a fixed RF sweep width, does not change the basic resolution capability but does change the range scale. The 150 millisecond sweep produced a smoother curve because it resulted in a better match between the sweep duration and the bandwidth of the filter in the spectrum analyzer used to process the difference frequency. The best resolution obtained with radar was 9-1/2 inches (24 cm) in air.

The range resolution was also measured by using as a target a block of "Rexolite" 1422 to simulate ice. Note that the dielectric constant of Rexolite (2.55) is reasonably close to that for ice (3.15). Figure 7 shows the radar return versus range obtained when the block of Rexolite was six inches (15.2 cm) thick. The front and rear surfaces of the block were easily detected. The velocity of propagation of radar waves through a medium is equal to that in free space divided by the square root of the dielectric constant of the medium, i.e.,

$$c_m = \frac{c}{\sqrt{\xi}}$$

where

$c_m$  = velocity of radar waves in medium

$c$  = velocity of radar waves in free space

and  $\xi$  = dielectric constant of medium

Therefore the transmission time through the six inch (15.2 cm) block of Rexolite was equal to the transmission time through 9.6 inches (24.4 cm) of free space.

Figure 8 shows the corresponding curve obtained with a 15" (39.1 cm) block of Rexolite as the target.

### 3.2 WATER ATTENUATION MEASUREMENT

The measurement of the thickness of the ice cover on a lake or river by radar may be complicated by a layer of water lying on the surface of the ice or at some depth within the ice.

Reference 2 indicates that the attenuation of an X-band wave in water is about 50 dB per centimetre. Thus, even a thin layer of water on top of or in the ice may reduce the amplitude of the return from the bottom surface of the ice to a level which is undetectable in the presence of the strong reflection from the water layer. In order to verify the high attenuation levels given in Ref. 2 an experiment was set up in the laboratory.

Three plastic receptacles were fabricated which would allow attenuation measurements through 1/16" (0.16 cm); 1/8" (0.32 cm); and 1/4" (0.64 cm) of water. After having been filled with water, each receptacle was placed against the face of the receiving horn antenna to ensure that all of the received power measured had passed through the water. The test set-up is shown in Figure 9 and the results are given in Table 1.

TABLE 1  
*Attenuation Measurements*

Water Depth	Measured Attenuation (dB)	Calculated Attenuation (dB)	Difference
1/16" (0.159 cms)	13.8	8.0	5.8
1/8" (0.316 cms)	22.2	15.9	6.3
1/4" (0.635 cms)	37.6	31.8	5.8

The column headed "calculated attenuation" shows the expected attenuation in the specified thickness of water. This does not include the reflective loss which is accounted for by the approximate 6 dB difference between measured attenuation and that calculated from Ref. 2. In the radar case the wave must pass through the water twice and the loss will be doubled. The attenuation which can be tolerated depends on the range sidelobe level and dynamic range of the radar. With the present radar this will limit water layer thickness to about 0.1 cm but improvements will allow this figure to be at least doubled.



### 3.3 COMPARISON OF DIRECT RADAR AND TAPE RECORDED OUTPUTS

A Uher Model 4000 tape recorder was added to the system so that all data obtained during field tests could be stored and retrieved in the laboratory for data analysis. The tape recorder was operated with a tape speed of 4.75 cm/sec.

A corner reflector (Figure 4) was placed in the radar range and this target was illuminated by the radar. With SW1 at position 3 (Figure 1) the target return signal was simultaneously recorded on the tape recorder, processed in the wave analyzer, and charted on the pen recorder. The wave analyzer output trace is shown in Figure 10a. With SW1 in position 1, the tape recorded video was then processed in the wave analyzer and the chart recorder output is shown in Figure 10b.

The curves presented in Figure 10a and 10b show a good similarity. The amplitude of the target return appears slightly greater in Figure 10b than that in Figure 10a; however, this is a function of the tape recorder gain setting.

### 3.4 COMPARISON OF RADAR AND DIGITAL RECIRCULATOR OUTPUTS

To test the performance of the digital recirculator, a block of Rexolite, nine inches (22.9 cm) thick, was placed in the radar range as a target. With the target illuminated by the radar and SW1 in position 3 (Figure 1) the video signals were processed by the wave analyzer and plotted on the pen recorder. The results are shown in Figure 11a.

While the run was in progress, the start button on the digital recirculator was depressed to activate the unit. Thus, a data sample was obtained during the actual run and stored in the recirculator. With the radar off and SW1 in position 2, the data stored in the recirculator was then processed in the wave analyzer. The pen recorder output is shown in Figure 11b.

The curves shown in Figure 11a and b have similar characteristics (except for amplitude) and the front and rear surfaces of the Rexolite block are clearly defined.

## 4. FIELD TESTS

### 4.1 RADAR MOUNTED ON SLED

Two field tests were attempted with the radar mounted on a sled towed by a snowmobile. The first series of tests were scheduled to be carried out on Lake Ontario at Wolfe Island on 1-2 February 1973. Unfortunately, because of a rapid rise in temperature and a heavy overnight rain which left a deep layer of water on the ice, this test had to be terminated before any useful data could be obtained.

The second field trial with the sled mounted radar was carried out on the Ottawa River on 15 February 1973. A map of the area, Figure 12, shows the approximate position of the three sites where stops were made and measurements carried out. The thickness of the ice was measured by the radar, and ice cores were taken to provide ground truth information. Ice thickness measurements were also made with the radar while in transit between the sites. A photograph of the sled-mounted radar is shown in Figure 13.

Figures 14 to 19 show the radar returns from the fixed tests (radar stationary) at the sites under various conditions. Except for Figure 16, these were produced by a digital computer from the recorded radar signals. The horizontal scale is the distance down from the radar antenna; each division represents ten centimetres for the expected radar wave propagation velocity in ice. The vertical scale is the amplitude of the radar return signal reflected from a target at the indicated range.

The following points should be considered in interpretation of the plots. First, the width of the peaks representing the strong returns from the ice surface and the ice/water interface is a function of the radar resolution capability. The basic resolution capability of the radar is somewhat better than is indicated by these plots; the resolution has been purposely degraded in the computer to compensate for some problems encountered in the field test. In addition, secondary peaks (usually referred to as "sidelobes") can be seen before and after the main peaks. These sidelobes are not due to reflections at the points indicated, but are generally a result of characteristics of the radar. The observation of higher sidelobe levels in the field data (Figure 14 - 19) than in the reported laboratory data appears to be due to the portable power source. The two true reflections that occur in Figure 14 at approximate ranges of 200 cm and 280 cm indicate an ice thickness of 80 cm which agrees well with the core depth. The small peak occurring about 20 cm before the return from the water is a sidelobe and does not indicate an internal reflection in the ice.

Figures 14 and 15 respectively show the returns at Site 1 before and after removal of the 2.5 cm thick snow cover on the ice. The snow appears to have reduced the reflections from the ice surface. In both cases an ice thickness of about 80 cm is indicated. The radar measurement compares well with the measurement (76.5 cm) obtained at this site.

At the fixed sites, long enough records were taken to allow processing of the signal on the low speed spectrum analyzer. Figures 16A and B show the signals processed in this way for Site 1. The processed range trace obtained after removal of the surface snow is shown in Figure 16A; the corresponding trace obtained after removal of the core of ice is shown in Figure 16B. After removal of the core, the water surface (about 2.5 cm below the ice surface) provided a strong reflection. The resolution of these plots was not reduced as it was in the computer generated ones. The apparent returns between 5 and 10 divisions from the left were caused by the power supply. In the computer generated plots, these false returns have been removed.

The peak which appears before the sidelobes of the ice-water interface return seems to coincide with the commencement of bubble-free clear ice at a depth of approximately 50 cm. This coincides also with the start of high density columnar ice as shown in Figure 21 which refers to Site 2. However,

the ice structure was similar at the two sites. This peak at 50 cm does not show up in the computer plot due to the proximity of the sidelobe from the lower surface and the lower resolution selected for the computer processing.

Figures 17, 18 and 19 show computer-generated plots of the results obtained at Site 2. In Figure 17, the surface snow was left untouched and the surface return appears broadened with the peak occurring at an approximate range of 225 cm. The actual surface was expected to be at a range of 200 cm as before and this was verified in Figure 18 when a metal plate was placed on the surface to provide a good reflection at that point. If the surface position is taken from Figure 18, the ice thickness at Site 2 was 75 cm which was in good agreement with the actual ice core removed at that site. The main return in Figure 17 appears to be from a point about 25 cm below the ice surface and this return masks the surface return to some extent. The plot shown in Figure 19 was obtained when the surface snow was removed from the ice. Little difference was apparent except that the amplitude of the surface reflection was reduced slightly.

For the analysis of the ice cores the cores were cut lengthwise in half. A second cut was made parallel to the first cut, resulting in a rectangular plate of about 2 cm thickness. Such a section from the ice core taken at Site 2 is shown in Figure 20. The top of the core is on the left side of the photograph. The first 32 cm of core represent superimposed ice, which formed by freezing of flooded snow. Below the 32 cm mark secondary ice formed to a depth of 74.0 cm. Some bubbles do appear near the top of the secondary ice. In Figure 22 the density has been plotted for the Site 2 core.

The plot shown in Figure 23 which was produced by the low speed spectrum analyzer (at the resolution of the radar) shows one peak which may be due to an internal reflection. With the higher resolution of this plot the broad peak which corresponds to the ice-snow surface in Figure 17 is separated into two peaks, one at the correct ice surface position as indicated in Figure 18 and a second about 30 cm below the surface. This seems to coincide with the boundary at a depth of 32 cm which separates the superimposed ice from the secondary ice. Although the higher resolution was useful in this case the degradation of the signal due to antenna motion and poor power supply characteristics made the resolution reduction as used in Figures 14 to 19 a desirable technique in most cases. The antenna motions were more severe than anticipated as a result of the long boom and bumpy ice. However, these motions can be accommodated, without degradation, by an adjustment in the radar parameters, and future radars will be able to provide the benefits of higher resolution.

The computer plots showing the results of the measurements taken at Site 3, Figures 24 and 25, are similar to those obtained at Site 2. The use of the metal plate (Figure 25) shows the true ice surface position and the measurements indicate an ice thickness of approximately 70 cm at this site.

Measurements were made with the sled in motion between the sites. Typical computer-generated plots of these results are provided in Figure 26. Successive measurements are plotted one below the other and the time interval between curves is 0.74 seconds. In each curve the vertical direction represents amplitude of reflection. The horizontal scale indicates the range downward from the radar antenna, each division representing 10 cm in ice. Motion

of the antenna, resulting from violent pitching of the sled as it crossed bumps, caused degradation of many of the curves. In spite of the problems encountered, the plots allow reasonably good estimates of ice thickness.

#### 4.2 RADAR MOUNTED ON AIR CUSHION VEHICLE (ACV)

Two field tests were carried out with the radar mounted on a Department of Environment ACV, one on the ice of Lake Ontario near Kingston, 6-8 March 1973, and a second on the Ottawa River, 14-16 March 1973. The results obtained from both tests were disappointing because of poor ice conditions. Slush and water covered the ice surfaces throughout the test periods.

The method used in mounting the horn antenna on the ACV is shown in Figure 27. The radar was housed in the cargo compartment and covered by a canvas canopy. In this photograph the hovercraft is sitting on the ice with all power off. Figure 28 shows the airborne ACV at the start of the run. The height of the antenna from the ice surface was increased by about 10 inches (25 cm) when the hovercraft was airborne with the skirt inflated. This height or range increase was quite noticeable on the ice measurement plots. The wet ice surface is apparent in both photographs.

A map showing the two test areas on Lake Ontario is given in Figure 29. In the first test, the hovercraft travelled from Wolfe Island to Kingston (Leg 1), Kingston to Snake Island (Leg 2), Snake Island to Lucas Point (Leg 3) Lucas Point towards Garden Island (Leg 4), and from the Wolfe Island ferry dock to the launching site (Leg 5). In the second test the ACV, launched at Button Bay on the south shore of Wolfe Island, travelled down Button Bay, rounded Hinckley Point and proceeded westward to a DOE test site on the ice opposite Cape Vincent, USA.

Typical computer plots of the results obtained during the tests with the ACV are shown in Figure 30. The main peak is due to the reflection from the upper ice surface. Little evidence of the reflection from the ice-water interface was found on the plots because of the poor penetration of the wet ice surface by the radar waves.

An ice core taken during the tests is shown in the photograph of Figure 31. The core is composed of vertical ice crystals instead of the solid ice previously observed. The surface of the ice was very pitted, as shown in the photograph. It is understood that this ice condition occurs during the mild sunny weather just prior to break-up. It is not known what effect the vertical ice crystals would have on the radar waves penetrating the ice surface.

The plots of Figure 30 show clearly the difference in height of the antenna when the ACV is airborne and when it is down on the ice surface. The surface return has moved to the left by approximately 16 cm (27 cm when converted to range in air) which corresponds to the change in antenna height.

The final test with the ACV was carried out on the Ottawa River. Unfortunately the ice was covered with 3-4 inches (8-10 cm) of wet slush and only rarely did the radar beam penetrate the ice surface. The results were disappointing and are not included in this report.

## 5. DOE ICE LABORATORY TESTS

Because of the unusual ice conditions encountered during the winter of 1972/73, additional laboratory tests were conducted under controlled conditions to test the equipment further. The experimental work to be described here demonstrates the measurement accuracy and resolution possible with the experimental radar, and also investigates the effect of surface water and snow layers upon the ability to measure ice thickness with the radar.

### 5.1 EXPERIMENTAL SET-UP

The equipment (Figure 3) was installed outside the cold room (as shown in Figure 32), to allow operation of the electronics at room temperature. The horn antenna was placed through a pre-cut hole in the cold room roof above the ice growing tank. Absorbing material was placed around the horn antenna inside the cold room to cut down on secondary reflections. The distance of the antenna to the ice surface was 1.4 m.

The 1.50 m diameter tank with a depth of 0.68 m is a quasi-permanent installation in a cold room where the temperature may be varied from 0°C to -30°C. The well insulated tank was filled with ordinary tap water and the cold room temperature set at -20°C. The vertical heat flow resulted in a planar ice-water interface as illustrated in Figure 32. Heating tapes, permanently installed between the tank insulation and the tank wall, were available to control the heat flow and ensure a planar interface, but their use was not required.

The dielectric properties of the laboratory-grown ice covers were measured at the frequency of the FM radar. These results are reported in Ref. 4. It suffices to mention that the dielectric constant was  $3.14 \pm 1.4\%$ .

Radar readings were taken two to three times a day after the ice had grown a few centimetres in thickness. To check the radar thickness measurements an ice thickness gauge (Ref. 3) was installed. The accuracy of this gauge was  $\pm 0.002$  m.

The ice grown in this tank was clear and no bubbles were visible to the naked eye. The crystal shape was columnar with a grain size of less than 0.01 m at the ice-interface.

### 5.2 EXPERIMENTAL RESULTS

#### 5.2.1 Ice Growth

A number of growth experiments were conducted throughout the summer months of 1973. Figure 33 shows the results of one of these experiments. The circles indicate the measurements made with the thickness gauge and the crosses the ones made by the radar. During the period of the experiment which started on 8 June and ended on 24 June 1973 the ice grew to a thickness of 0.33 m. The first useful radar measurements were obtained at a thickness reading of 0.15 m. The agreement between the two measurements is excellent: the error of thickness reading is of the order of  $\pm 0.01$  m. Similar results

were obtained from other tests. Based on comparison with the ice gauge, the minimum thickness that the radar configuration used here could measure was  $0.16 \pm 0.01$  m. This supports the previous estimate of 0.14 to 0.15 m, based on the radar resolution limit.

### 5.2.2 Water on Ice Surface

Since it is not unusual to have water on the surface of the ice, the radar was tested to determine the depth of water that would prohibit ice thickness measurements. Figure 34 shows the results of this test. The ice was at a temperature of  $-1.5^{\circ}\text{C}$  and the water which was added to the surface was at a temperature of  $2^{\circ}\text{C}$ . As the water was added to the surface, the signal amplitude from the surface return became greater while the signal amplitude from the ice-water interface return decreased. Due to the surface roughness of the ice, the water did not form a layer of uniform thickness over the entire illuminated surface. Small puddles formed, with some wet ice still being exposed to the radar. In general, however, the test verifies that wetting the surface gives rise to a stronger return from the surface of the ice and reduced return from the water-ice interface. Figure 35 shows how the wetted ice-air and ice-water interface amplitudes varied with the amount of puddled water and wet ice on the surface. The "water layer thickness" was obtained by dividing the total volume of water added to the surface by the area of ice coverage. Taking the uncertainty of water depth into account, the previously mentioned results in Section 3.2 agree with the general trend observed in this set of experiments. It is also clearly demonstrated how quickly the ice-water interface echo amplitude decreases as water is added to the surface. These tests show the desirability of having a slightly wetted ice surface to increase the surface echo amplitude. However too much water on the surface will quickly eliminate a return from the ice-water interface as mentioned in Section 3.2 and shown in Figure 35.

### 5.2.3 Snow on Ice Surface

In order to investigate the effect of surface snow on the performance of the ice-thickness measuring radar, the experiment described in 5.2.2 was repeated, using instead of water a layer of snow on the ice surface. The man-made snow, having a density of  $327 \text{ Kg/m}^3$ , was obtained from the Low Temperature Laboratory of the National Research Council. Figure 36 shows the effect of increasing snow depth upon the amplitude of the return from the upper ice surface. In agreement with the field observations, the ice surface peak return becomes less well defined as snow is added. Three centimetres of snow is sufficient to decrease the surface return amplitude by about 70%. A separate return from the snow surface became recognizable as the snow depth approached the radar resolution limit (about 0.14 m). The limited quantity of snow available made it impossible to investigate the effects of depths in excess of 14 cm.

## 6. SUMMARY

The laboratory tests have shown that the ice thickness can be measured accurately by this radar to within  $\pm 0.01$  m, with a minimum measurable average ice thickness of 0.16 m. A wet ice surface will enhance the surface return

and can be an advantage in field measurements. Snow, on the other hand, reduces the surface amplitude considerably.

The addition of the Uher tape recorder to the radar system satisfied the requirement for a means of data storage on the field trips. The stored data was retrieved without difficulty in the laboratory and processed on the Sigma 7 computer. The digital recirculator provided a means of measuring the ice thickness at any given point while the radar was in motion.

In the laboratory the radar had the capability of measuring the distance between two targets that were 9-1/2 inches (24 cm) apart. Since the velocity of radar waves in ice is only about 0.6 times their velocity in free space, the radar should have the capability of measuring a minimum ice thickness of 5-1/2 to 6 inches (14-15 cm).

Measurements of attenuation through water indicate that water layer depths in excess of about 0.1 cm on or in the ice would prevent ice depth measurement with the present radar. However, improvements in the radar to reduce range sidelobes should allow measurements with water layer depths of at least 0.2 cm.

No difficulty was encountered in mounting the radar system on either a sled or an ACV. A gasoline generator was used as a source of 110V 60 Hz power for the sled tests and two 12V storage batteries in conjunction with two DC to AC converters were used in the ACV tests. The gasoline generator presented no voltage fluctuation problems, but it is believed that the radar system was affected by the electrical interference from this power source. The electrical load on the two storage batteries was such as to limit radar operation to one hour periods per battery charge. In addition, the output AC voltage from the converters declined at a steady rate throughout the one hour period of operation. This decreasing supply voltage presented some problems in radar operation as it affected all parts of the system, particularly the sweep generator and TWT output tube.

As shown in Figures 27 and 28, the antenna boom was mounted over the two propulsion engines to allow the horn antenna to illuminate the ice surface immediately behind the ACV. The horn antenna should have been positioned further to the rear to eliminate any possibility of the radar illuminating the steering fins or the rear portion of the inflated ACV skirt. It is believed that electrical interference from the two propulsion engines (which were constantly being adjusted while the ACV was in motion) contributed to the extraneous noise that is visible on some of the plots. Time did not permit this problem to be investigated.

Of the four field tests carried out, only the Ottawa River test of 15 February 1973, with the radar mounted on a sled, could be termed successful. During the test the temperature was +15°F, and the ice was firm and hard (i.e., cold). The thickness of the ice, as measured by the radar consistently agreed with the length of the ice cores taken to provide ground truth information. In all other tests, the air temperature was above +32°F and the ice was wet and covered with either a layer of water or a 3-4 inch (8-10 cm) layer of wet slush. Only marginal results were obtained from these tests.

Vertical motion of the antenna can cause degradation of the radar response, resulting in the widening of the peaks and in the generation of range sidelobes. In the system used in this test, vertical velocities in excess of 2.5 ft/sec and vertical accelerations in excess of 0.2g will have this effect. Both of these values were greatly exceeded at times during the sled tests due to the pitching of the sled as it passed over irregularities in the ice surface. Many of the degraded curves are the result of sled pitching. The sensitivity to these motions is a function of the duration of the frequency sweep, and in a proposed airborne system, the sweep duration will be reduced to allow vertical velocities of up to 10 ft/sec and accelerations of up to 1g.

An improved version of this radar which will be much lighter in weight and will require much less primary power is being designed and constructed at CRC for use during the winter of 1973/74. The horn antenna will be replaced by a parabolic reflector three feet in diameter, to obtain an antenna beamwidth of 2.5°. Arrangements are underway for installing the radar in an MOT Jet Ranger helicopter prior to 1 December 1973. Flights will be made over the St. Lawrence Seaway throughout the winter to measure the thickness of the ice cover.

## 7. CONCLUSIONS

The tests described in this Technical Note have shown the feasibility of carrying out fresh water ice thickness measurements by radar from a moving platform. Successful measurements were carried out with the radar mounted on a sled and towed by a snowmobile. Some degradation of the radar response occurred as a result of the vertical motion of the antenna caused by pitching of the sled as it passed over irregularities in the ice surface. This problem can be overcome without difficulty by reducing the sweep duration of the transmitted waveform, thus allowing good measurements to be taken from an airborne platform.

Measurements with the radar mounted on a small ACV were less successful because of unsuitable weather conditions that resulted in a layer of water and slush on the ice surface. This confirmed our expectations that even a thin layer of water on the ice surface will prevent sufficient penetration of the ice by the radar wave to provide a measurable reflection from the bottom of the ice. Such conditions are not expected to occur over a large percentage of time during the winter.

## 8. ACKNOWLEDGEMENT

The authors wish to thank Messrs. R. Weaver, D. Cable and T. Bellaar Spruyt of the Department of the Environment for their assistance throughout the project.



## 9. REFERENCES

1. Venier, G.O. and F.R. Cross, *An Experimental Look at the Use of Radar to Measure Snow and Ice Depths*, CRC Technical Note 646, November 1972.
2. Royer, G.M., *Dielectric Properties of Microwave Frequencies of Ice, Snow and Water and the Measurement of the Thicknesses of Ice and Snow Layers with Radar*, CRC Report 1242, June 1973.
3. Ramseier, R.O. and R.J. Weaver, *Floating Ice Thickness and Structure Determination - Heated Wire Technique*, Department of the Environment, Inland Waters Directorate, Technical Bulletin 88, 1975.
4. Vant, Malcolm, *A Study of the Dielectric Behaviour of Fresh and Sea Ice at Microwave Frequencies*, Carleton University, Department of Electronic and Materials Engineering Technical Report, October 1973.

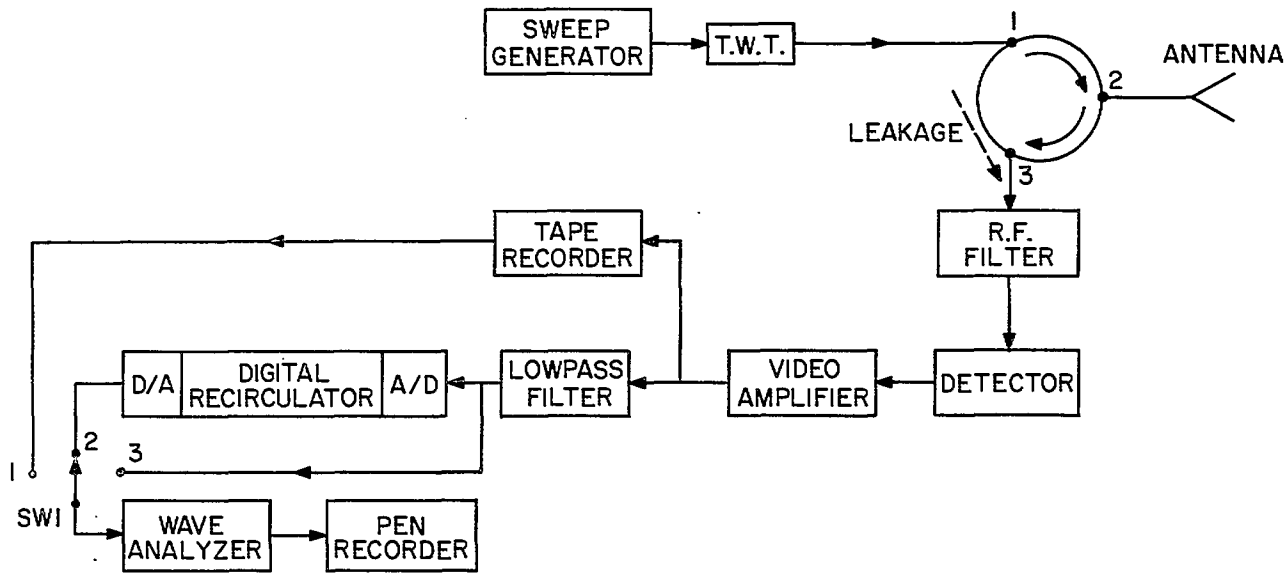


Figure 1. Block Diagram of Radar

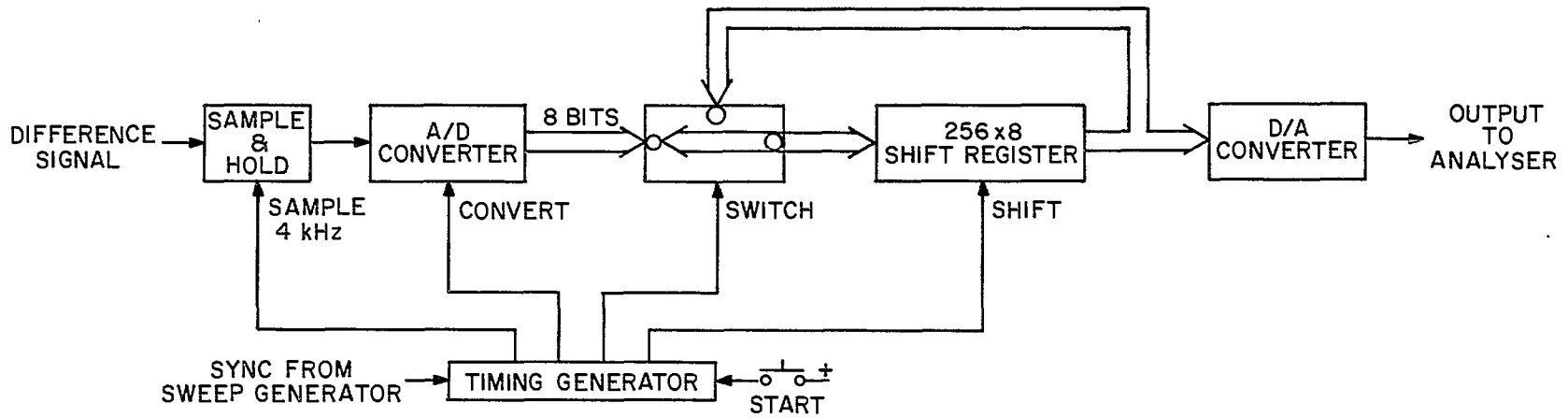


Figure 2. Block Diagram of the Digital Recirculator

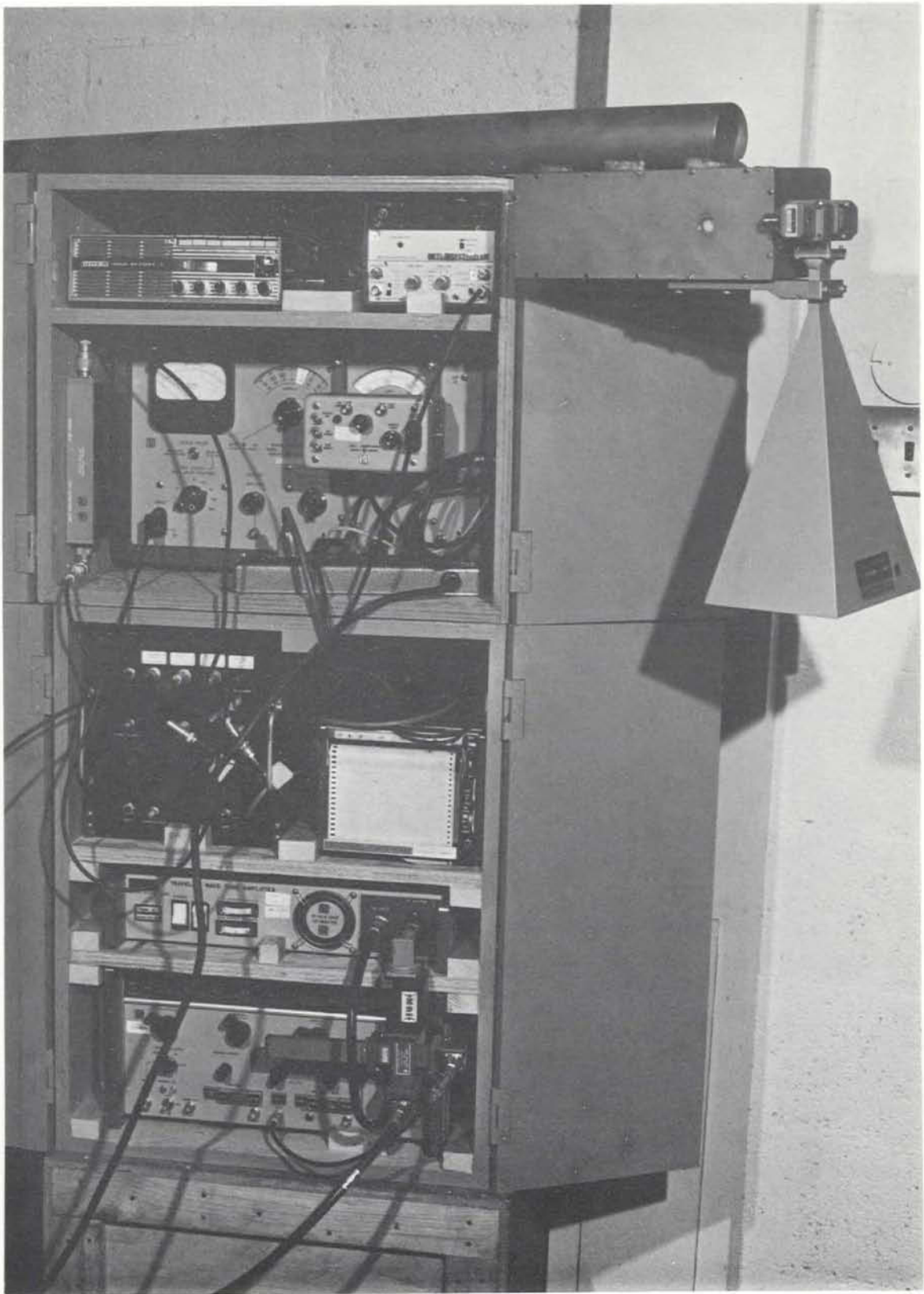


Figure 3. Photograph of Radar

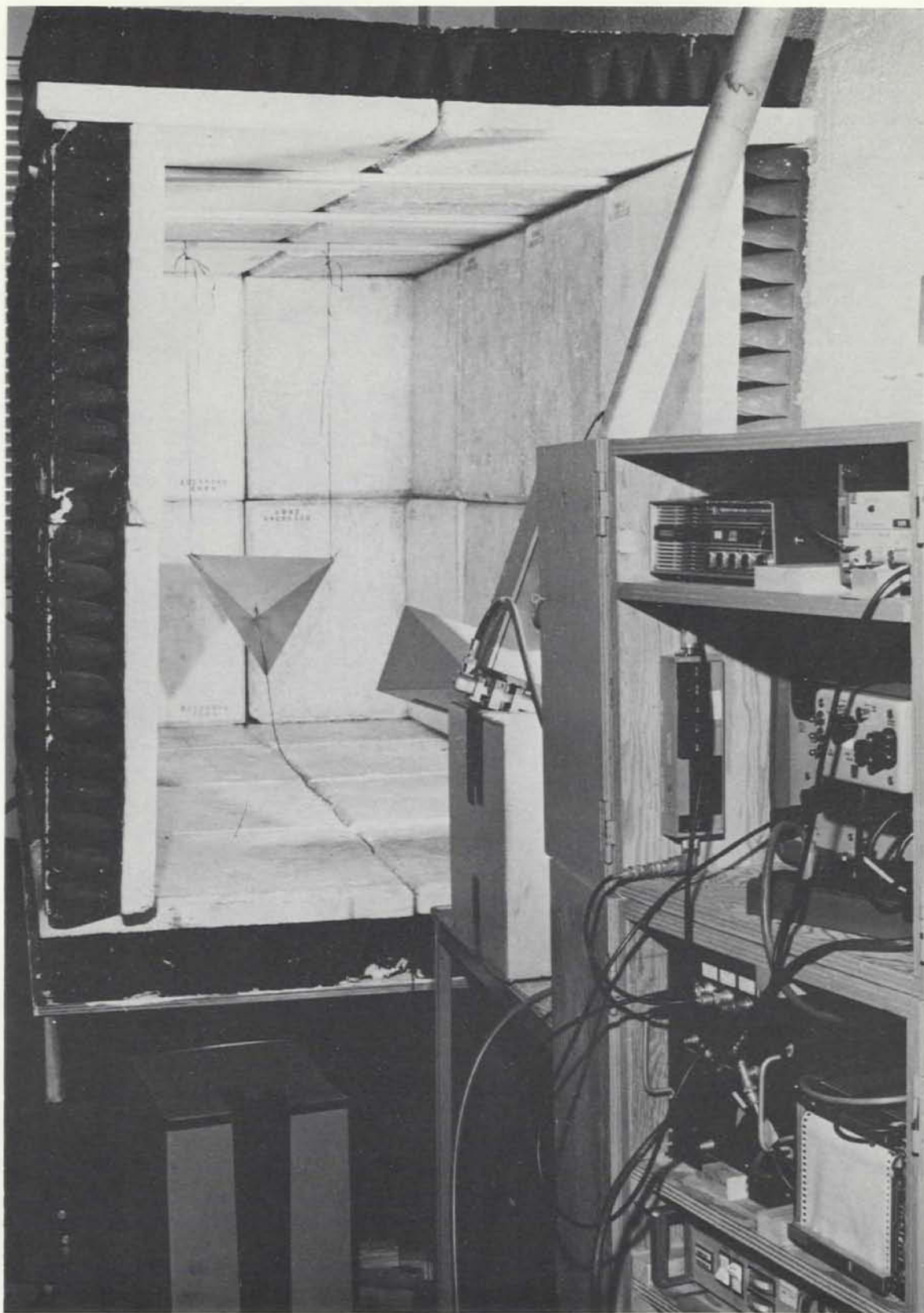


Figure 4. Photograph of Radar Range

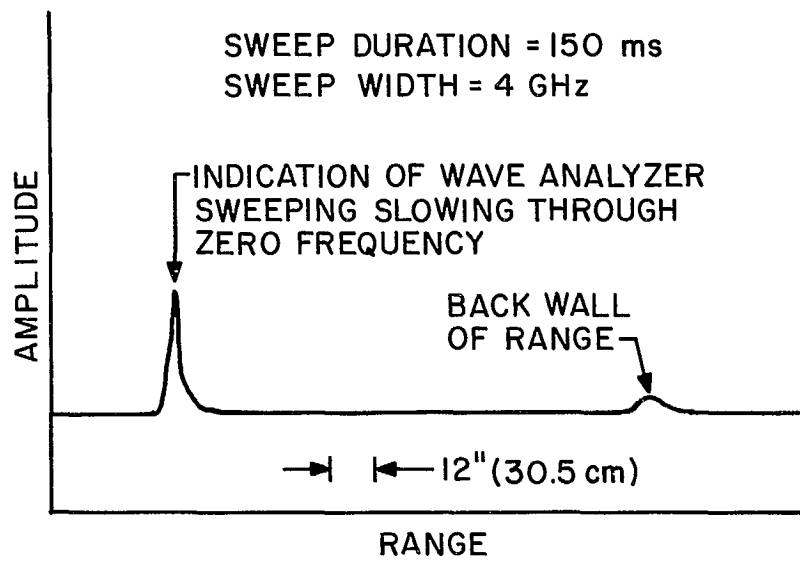


Figure 5. Radar Range Characteristics

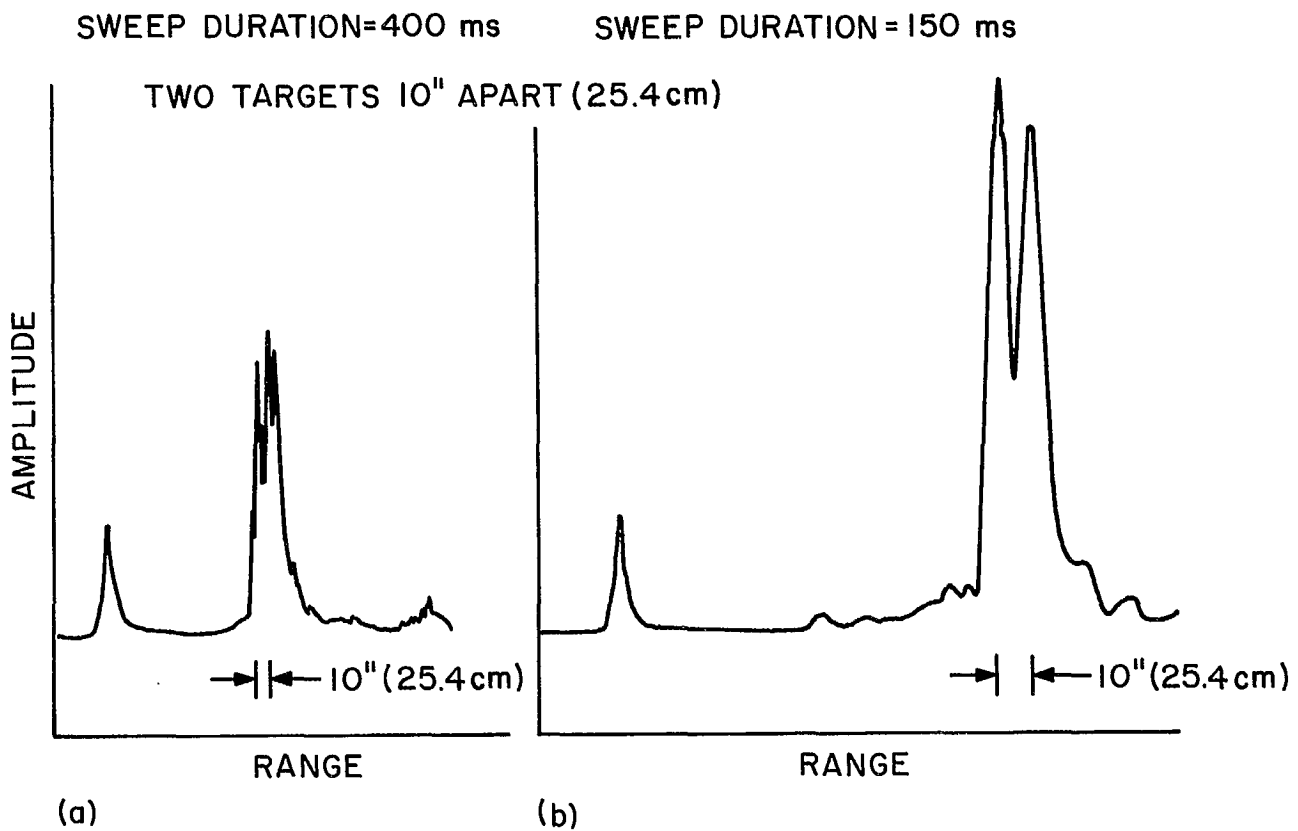


Figure 6. Radar Resolution Characteristics

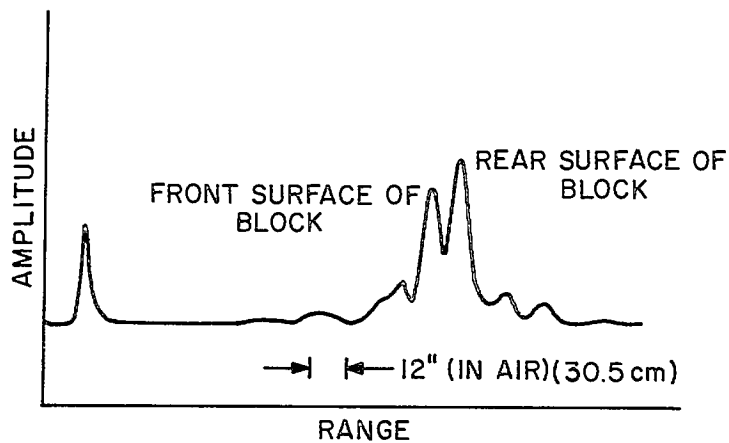


Figure 7. Radar Resolution Characteristic of a Six Inch Block of Rexolite

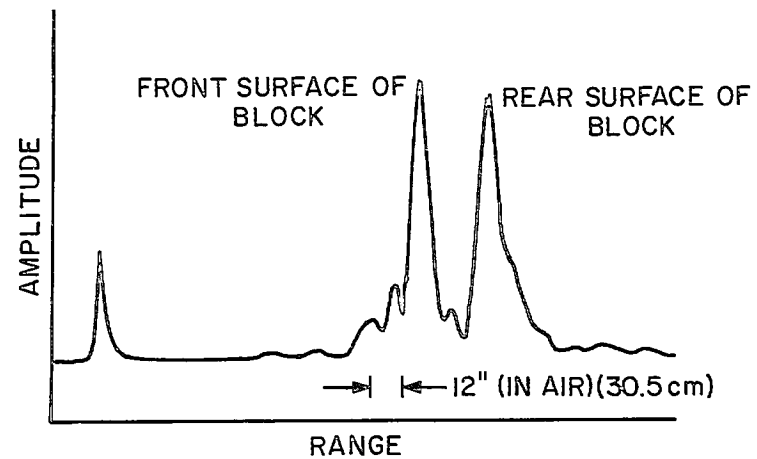


Figure 8. Radar Resolution Characteristic of a Fifteen Inch Block of Rexolite

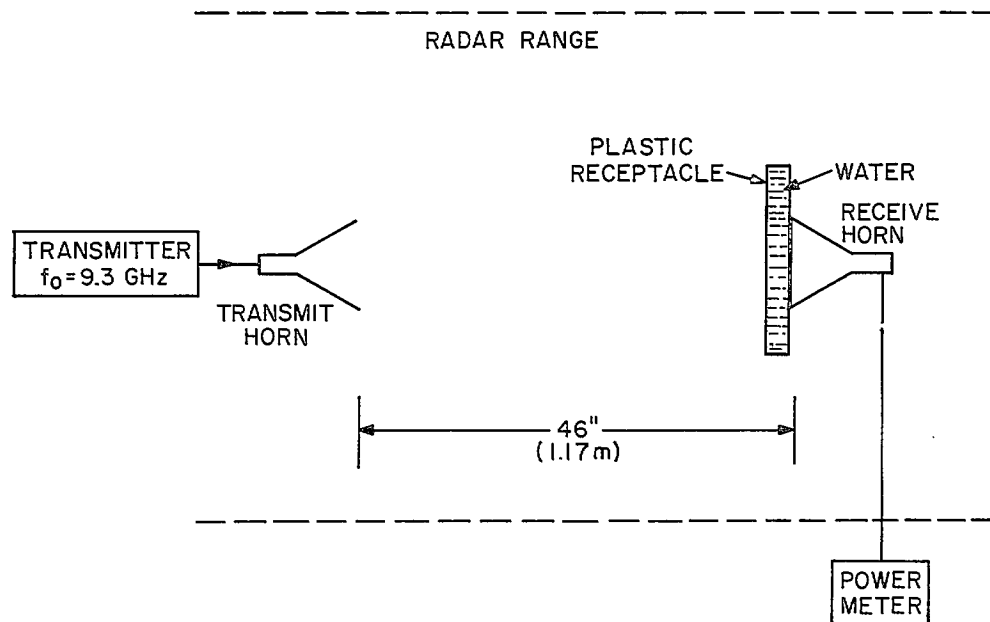


Figure 9. Test Set-up for Water Attenuation Measurements

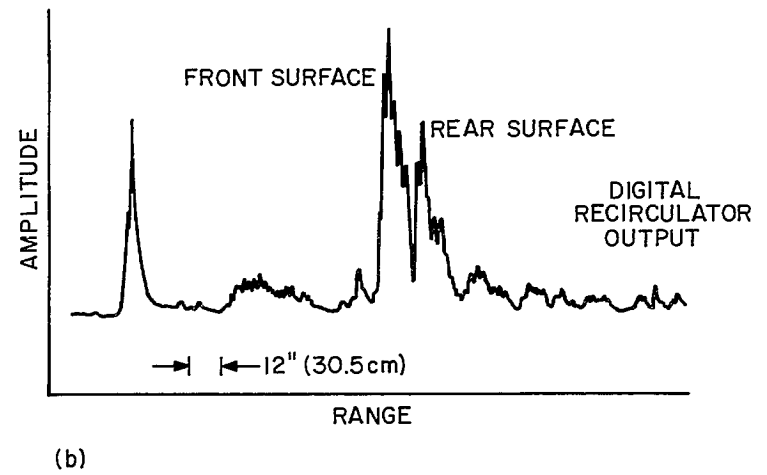
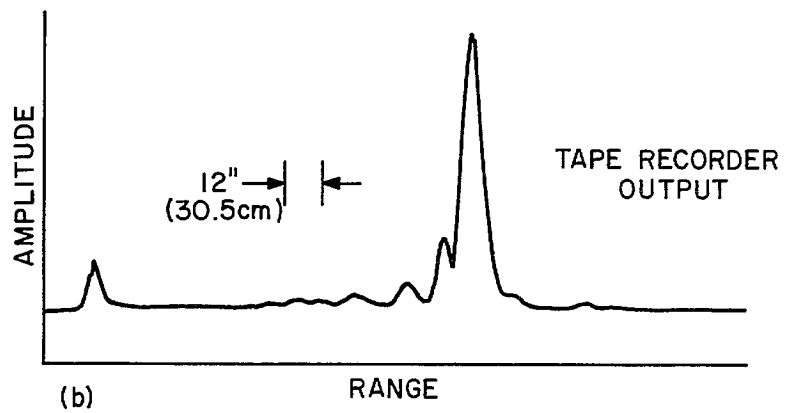
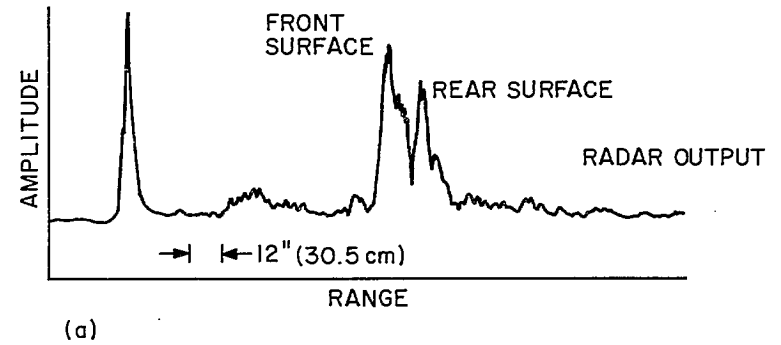
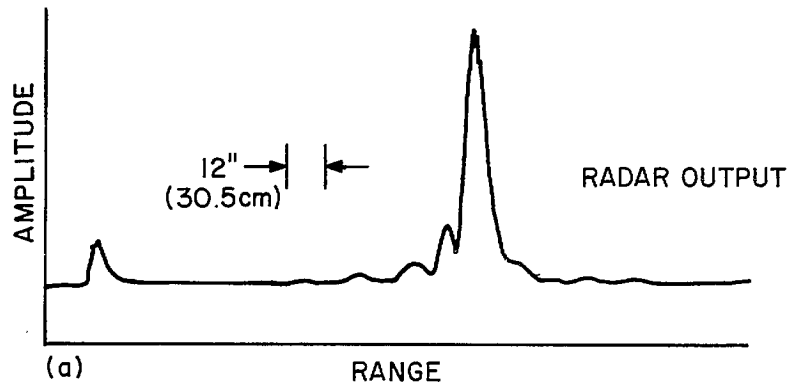


Figure 10. Comparison of Radar and Tape Recorder Outputs

Figure 11. Comparison of Radar and Digital Recirculator Outputs

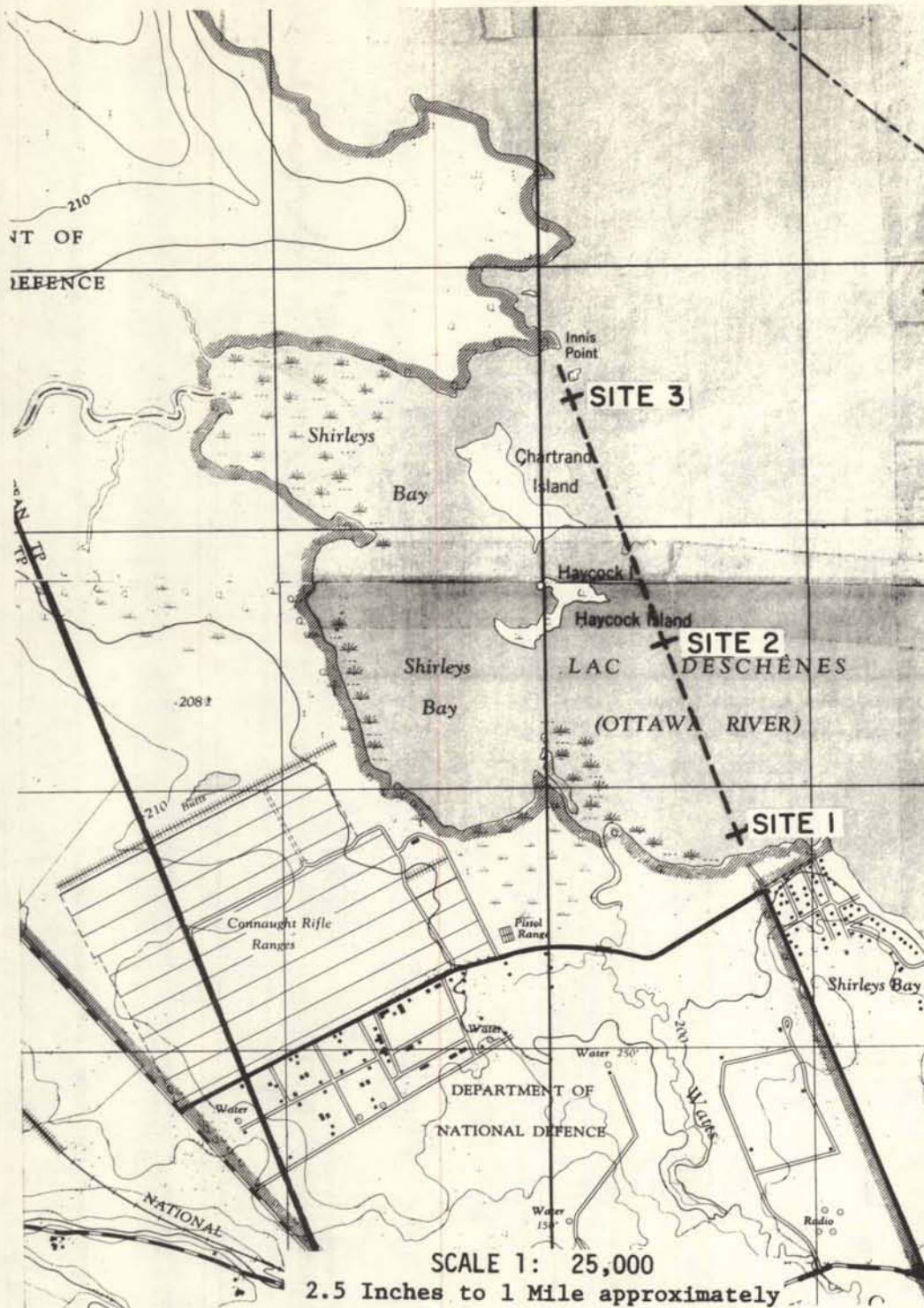
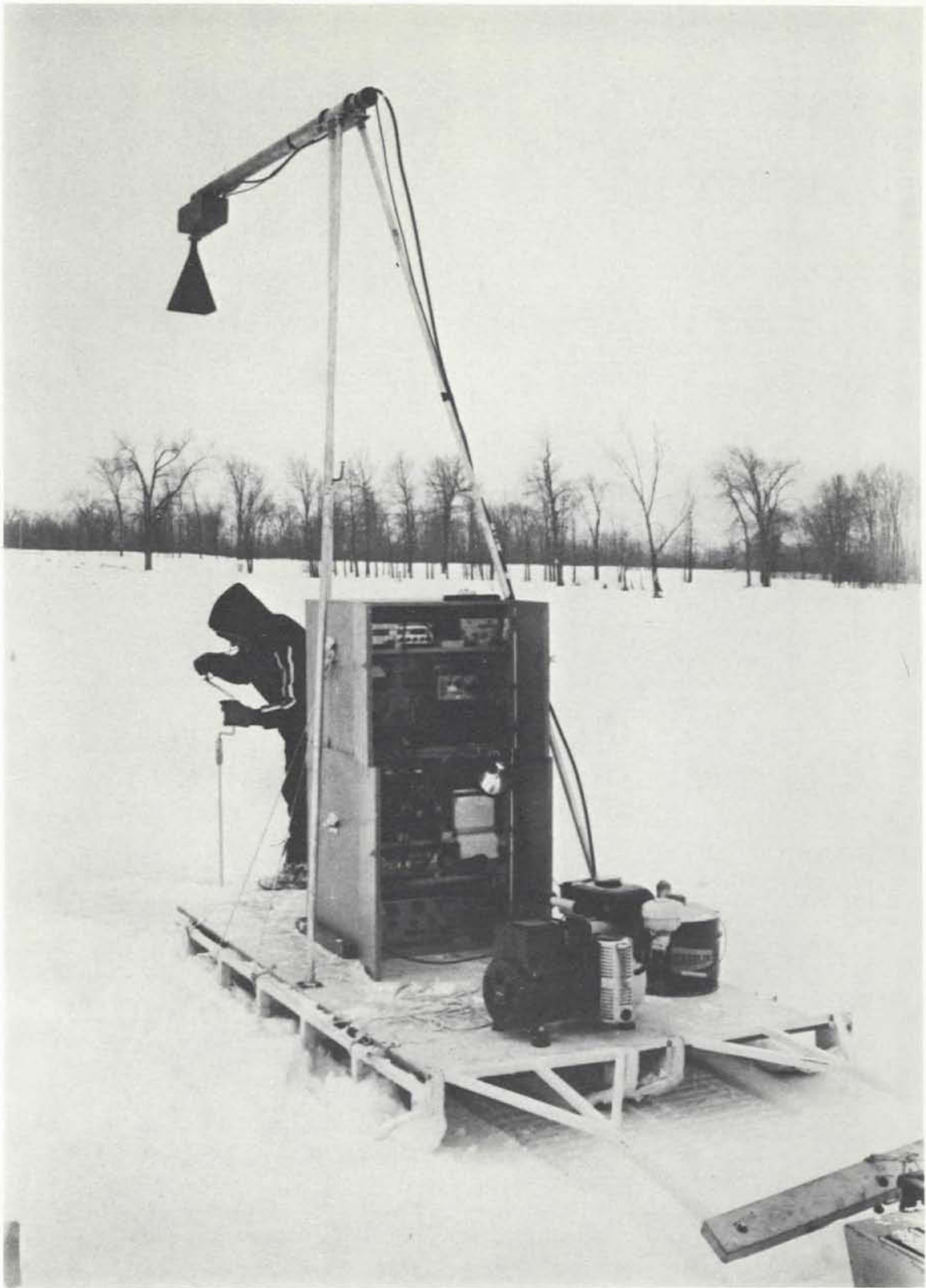


Figure 12. Ottawa River Test Area





*Figure 13. Photograph of Sled Mounted Radar*

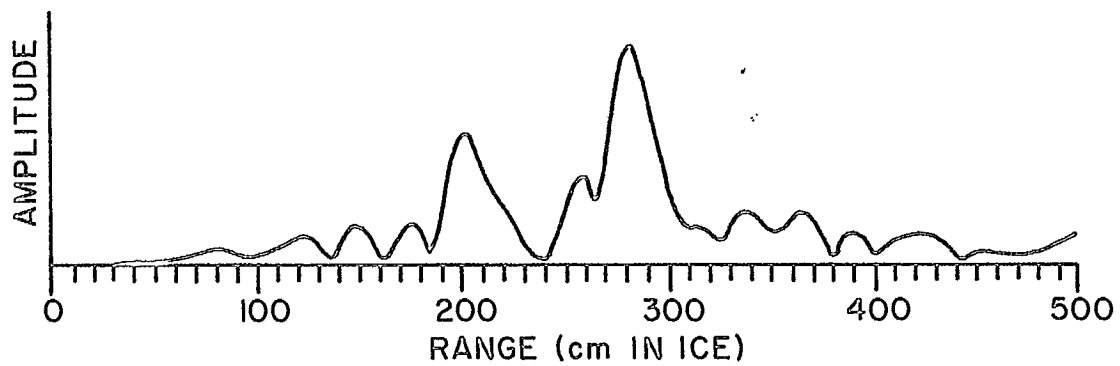


Figure 14. Computer Plot, Radar Return With Snow Cover, Site 1

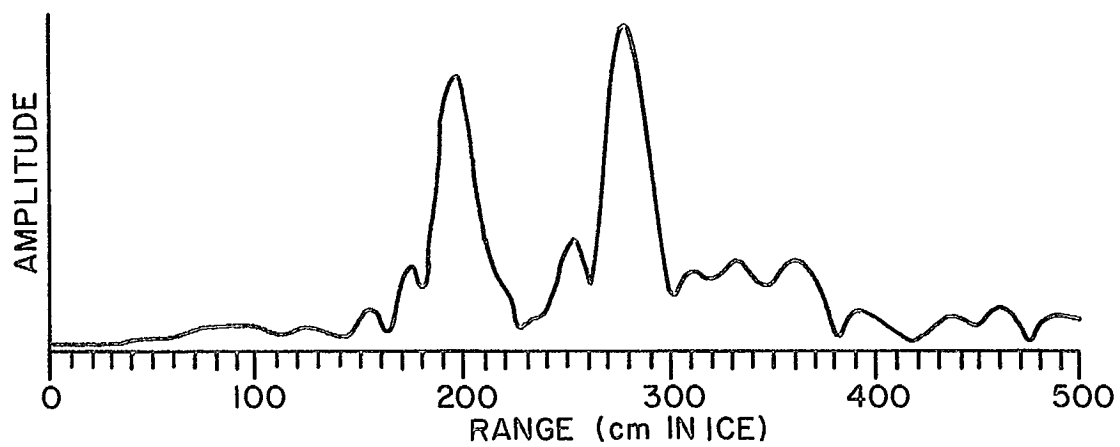


Figure 15. Computer Plot, Radar Return Without Snow Cover, Site 1

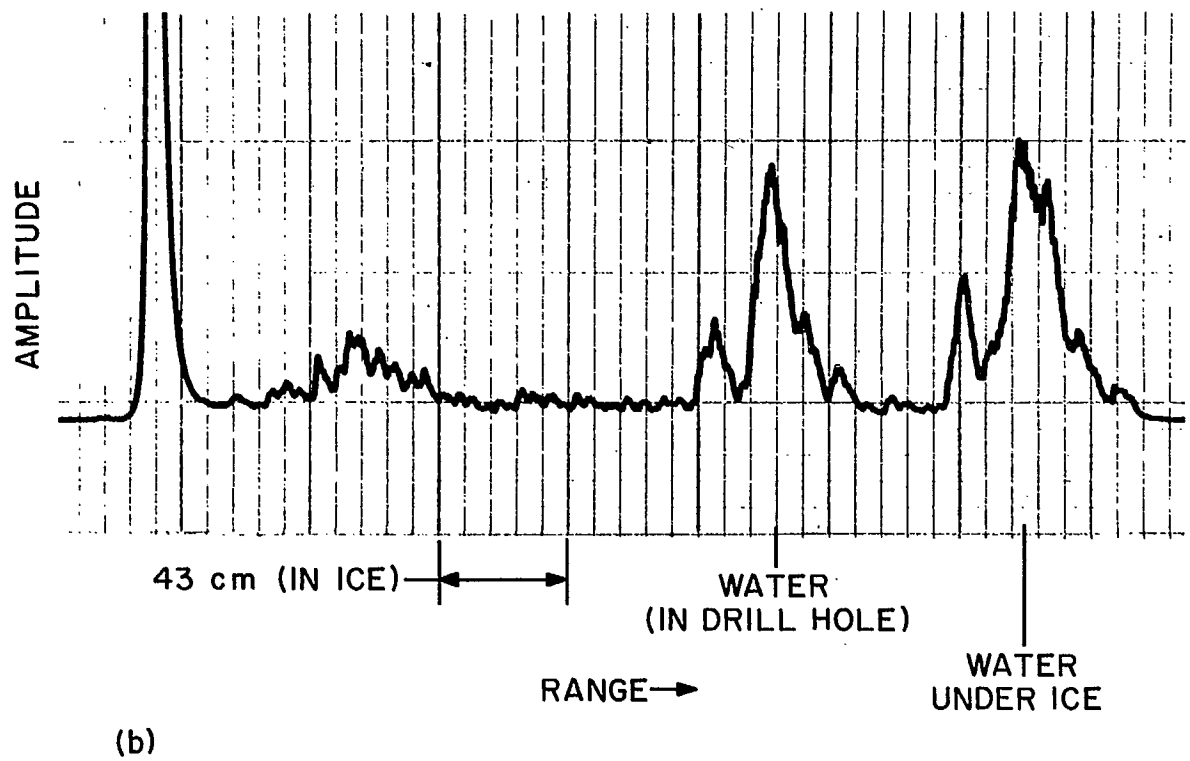
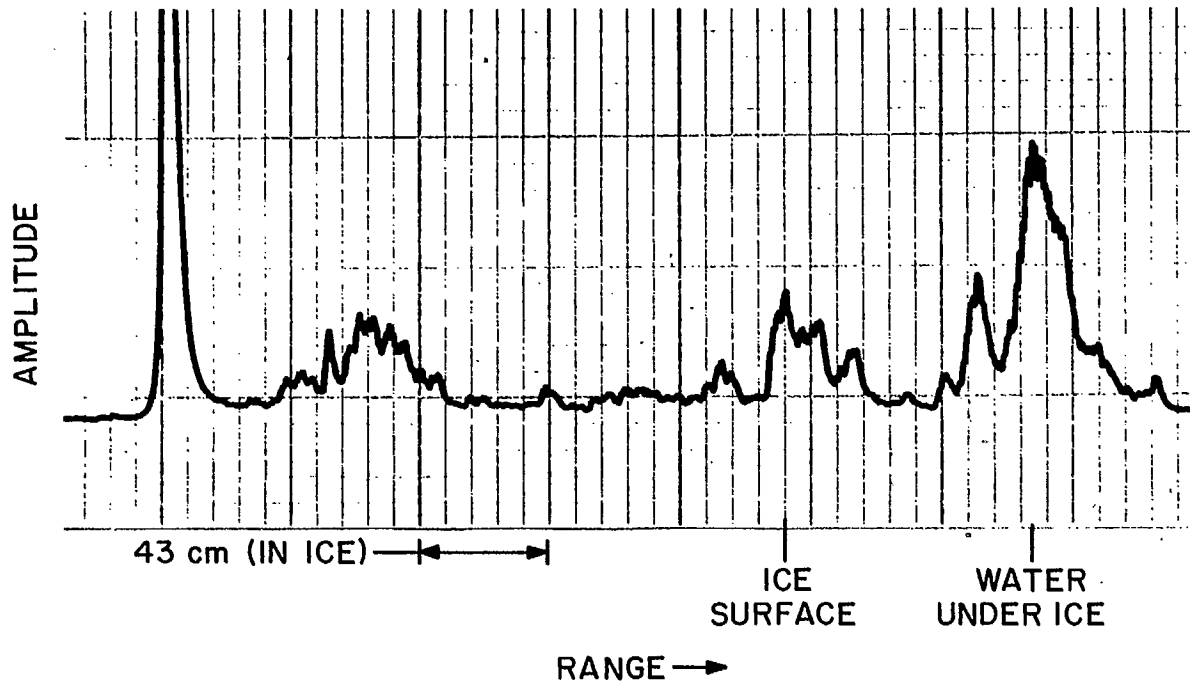


Figure 16. Low Speed Spectrum Analyzer Plot, Site 1

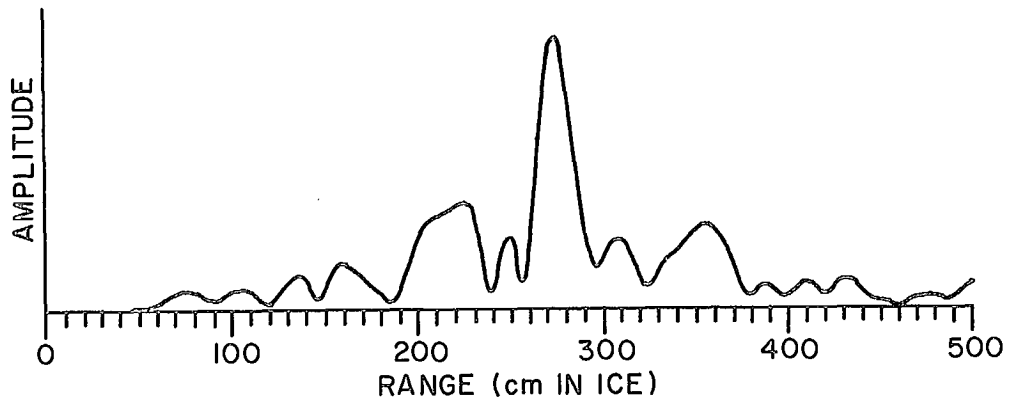


Figure 17. Computer Plot, Radar Return With Snow Cover, Site 2

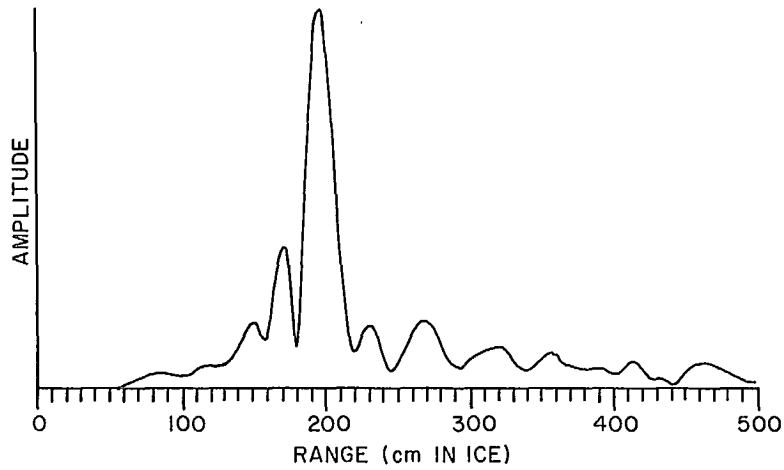


Figure 18. Computer Plot, Radar Return With Metal Plate on Ice Surface, Site 2

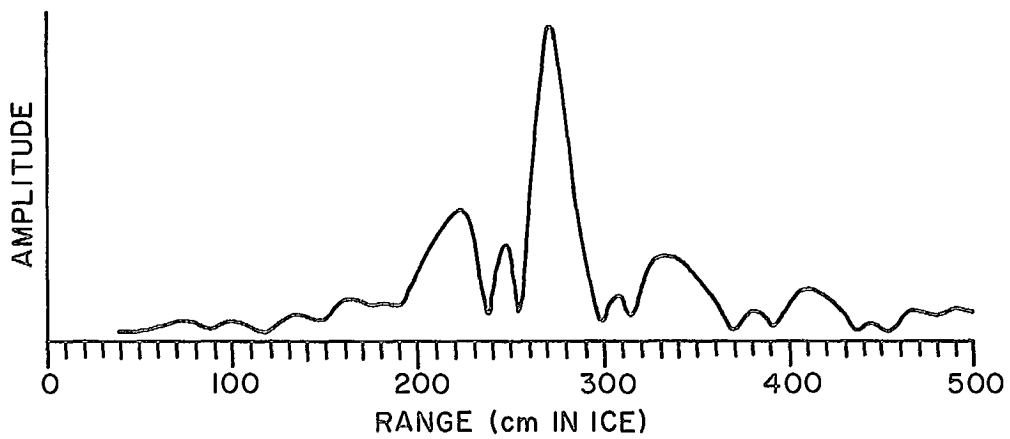


Figure 19. Computer Plot, Radar Return Without Snow Cover, Site 2

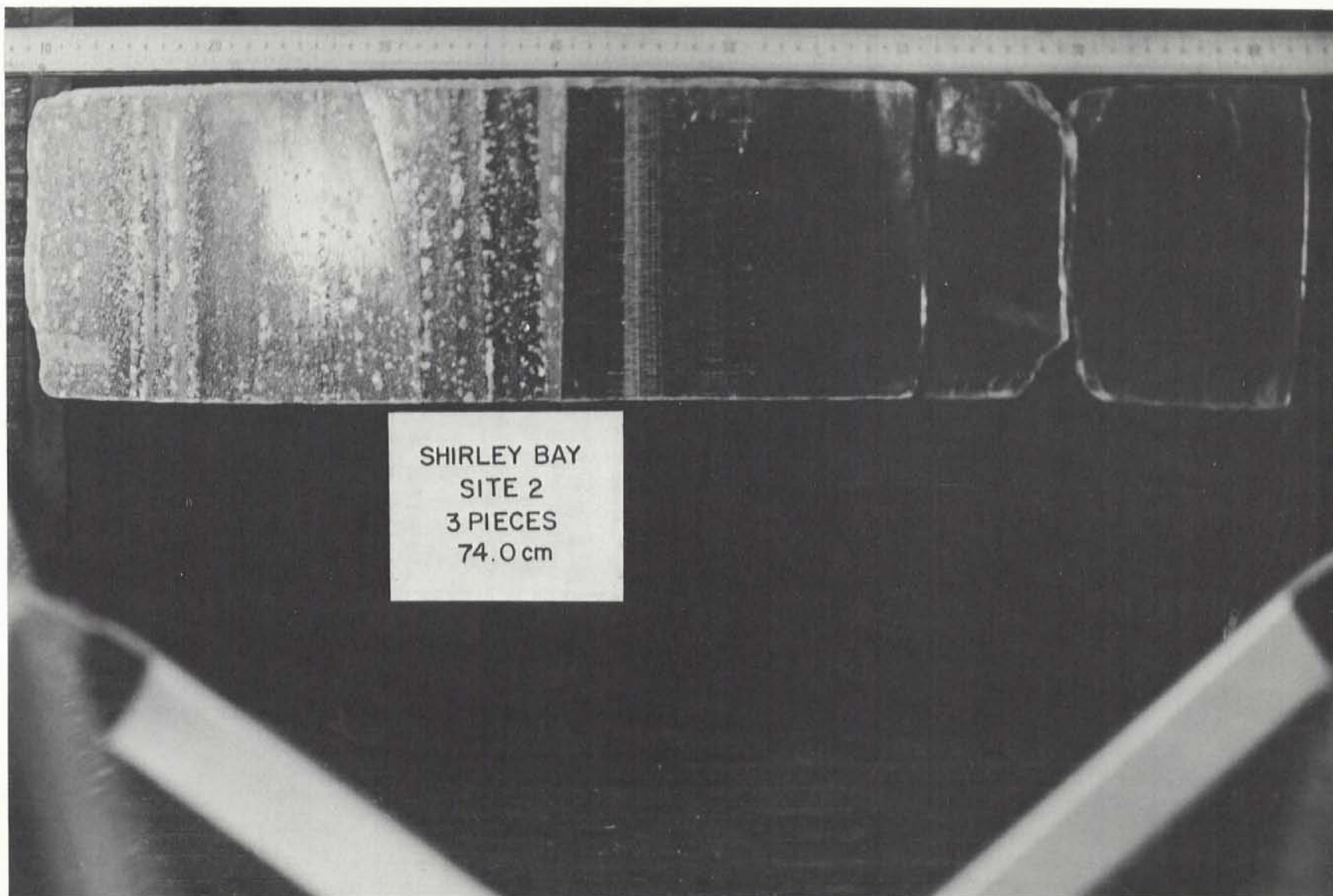


Figure 20. Sample Ice Core, Site 2

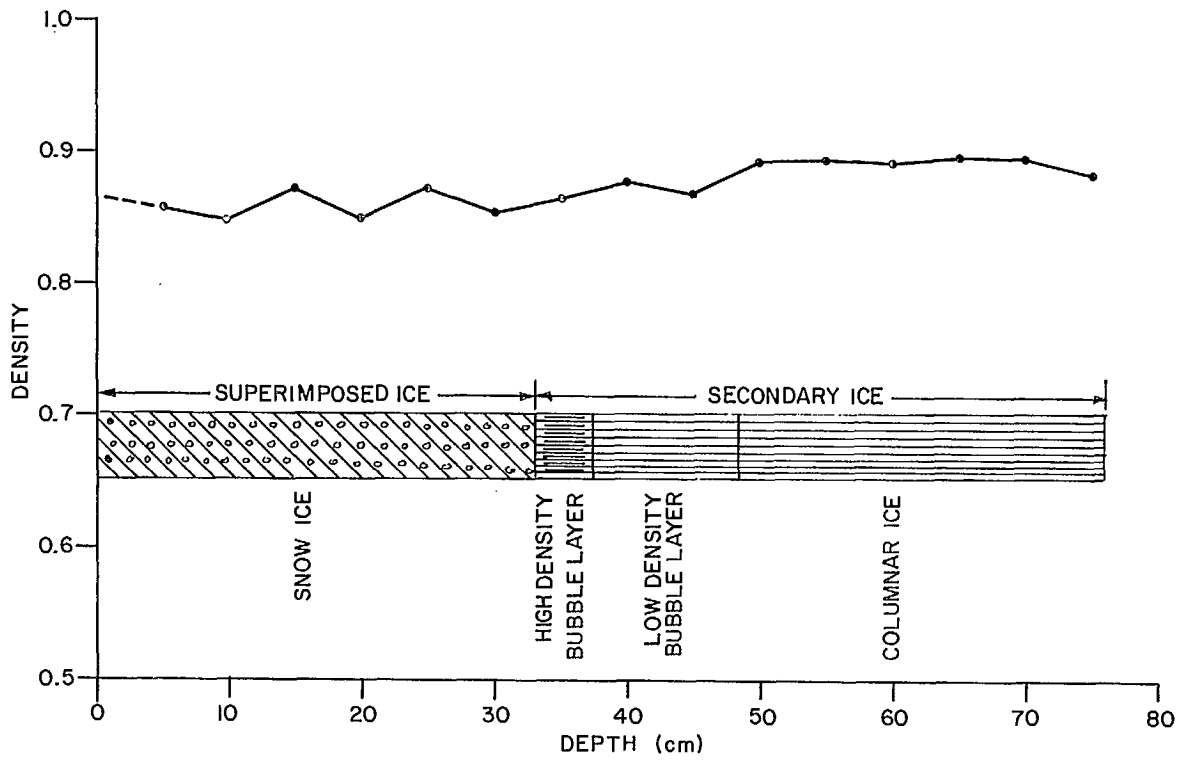


Figure 21. Ice Core Analysis, Site 1

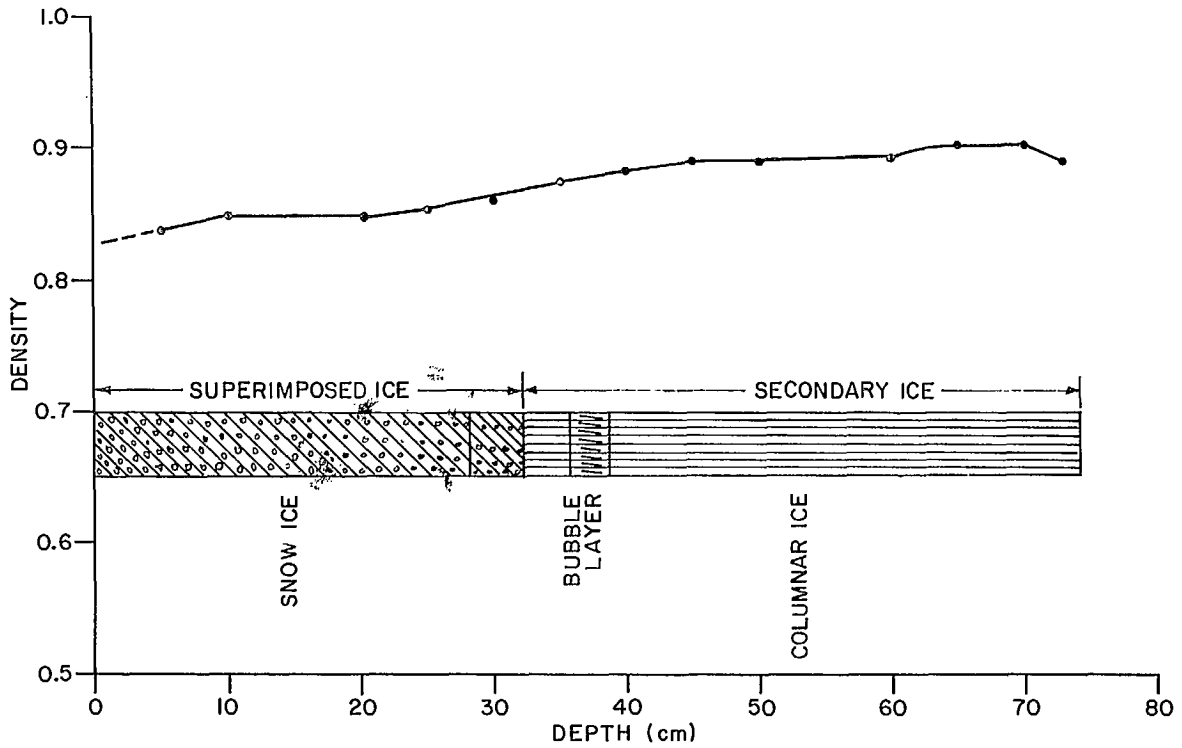


Figure 22. Ice Core Analysis, Site 2

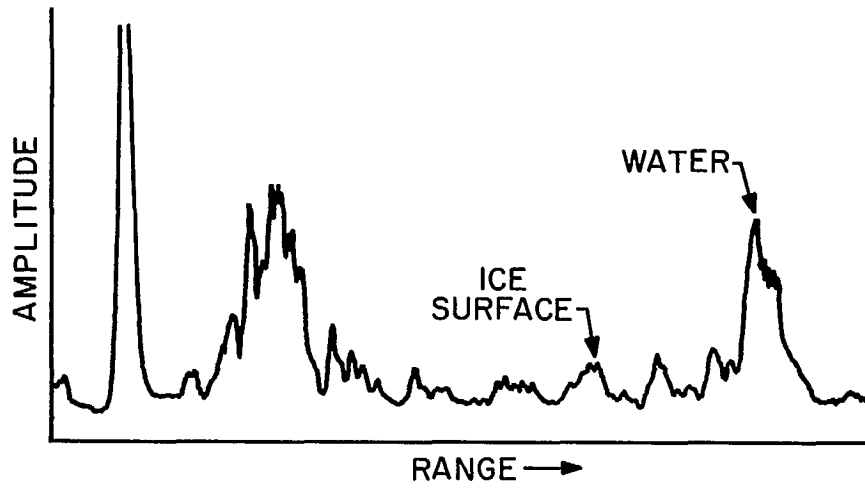


Figure 23. Low Speed Spectrum Analyzer Plot, Site 2

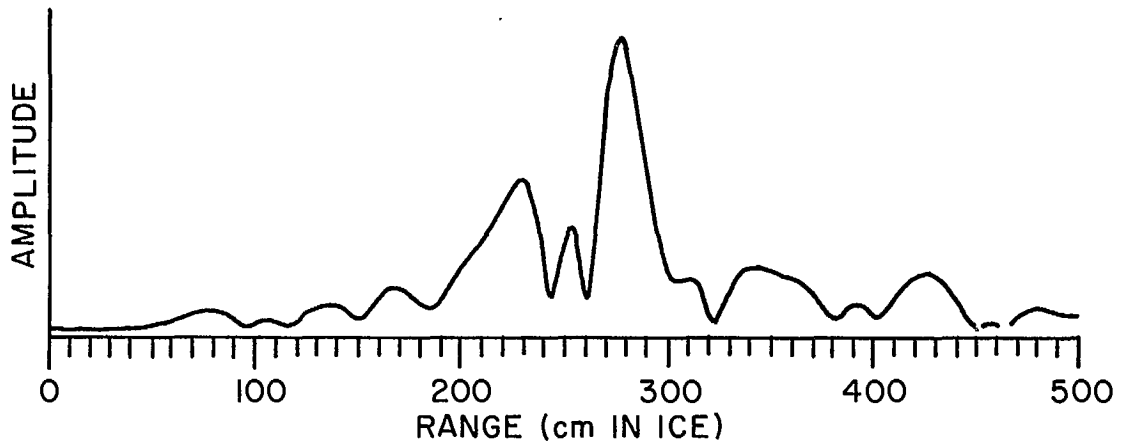


Figure 24. Computer Plot, Radar Return With Snow Cover, Site 3

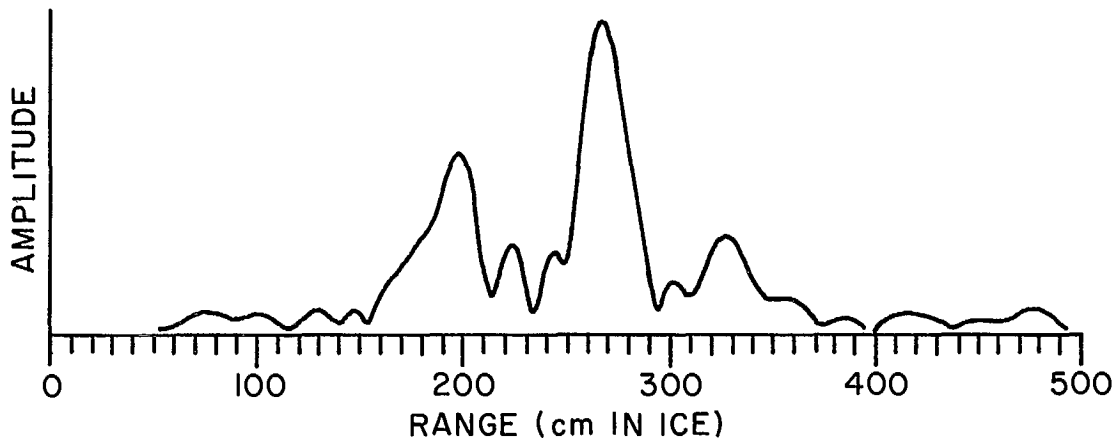


Figure 25. Computer Plot, Radar Return With Metal Plate on Ice Surface, Site 3

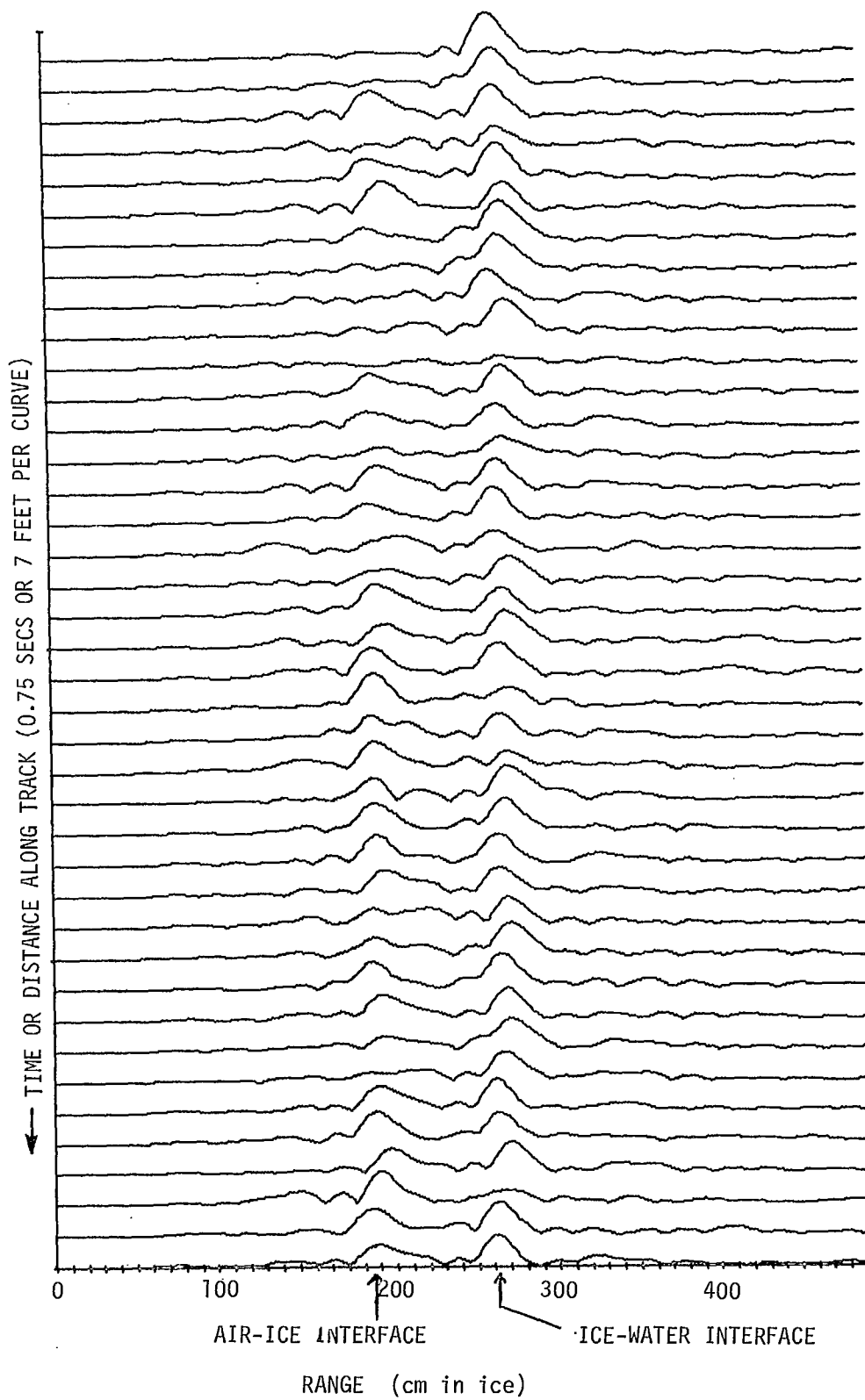


Figure 26. Computer Plot, Sled in Motion





*Figure 27. Radar Mounted on ACV*



Figure 28. ACV at Start of Test Run



Figure 29. Lake Ontario Test Areas

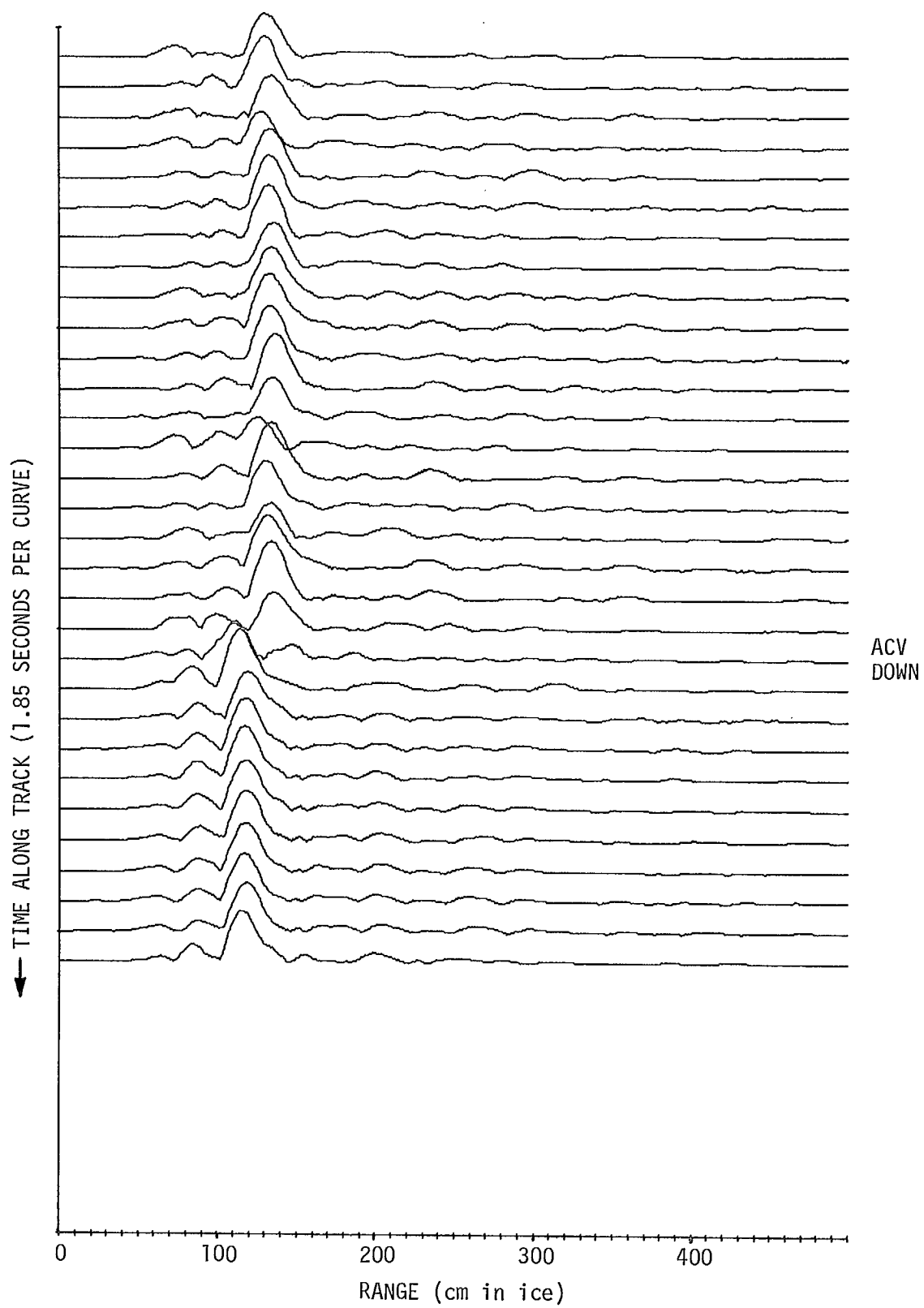
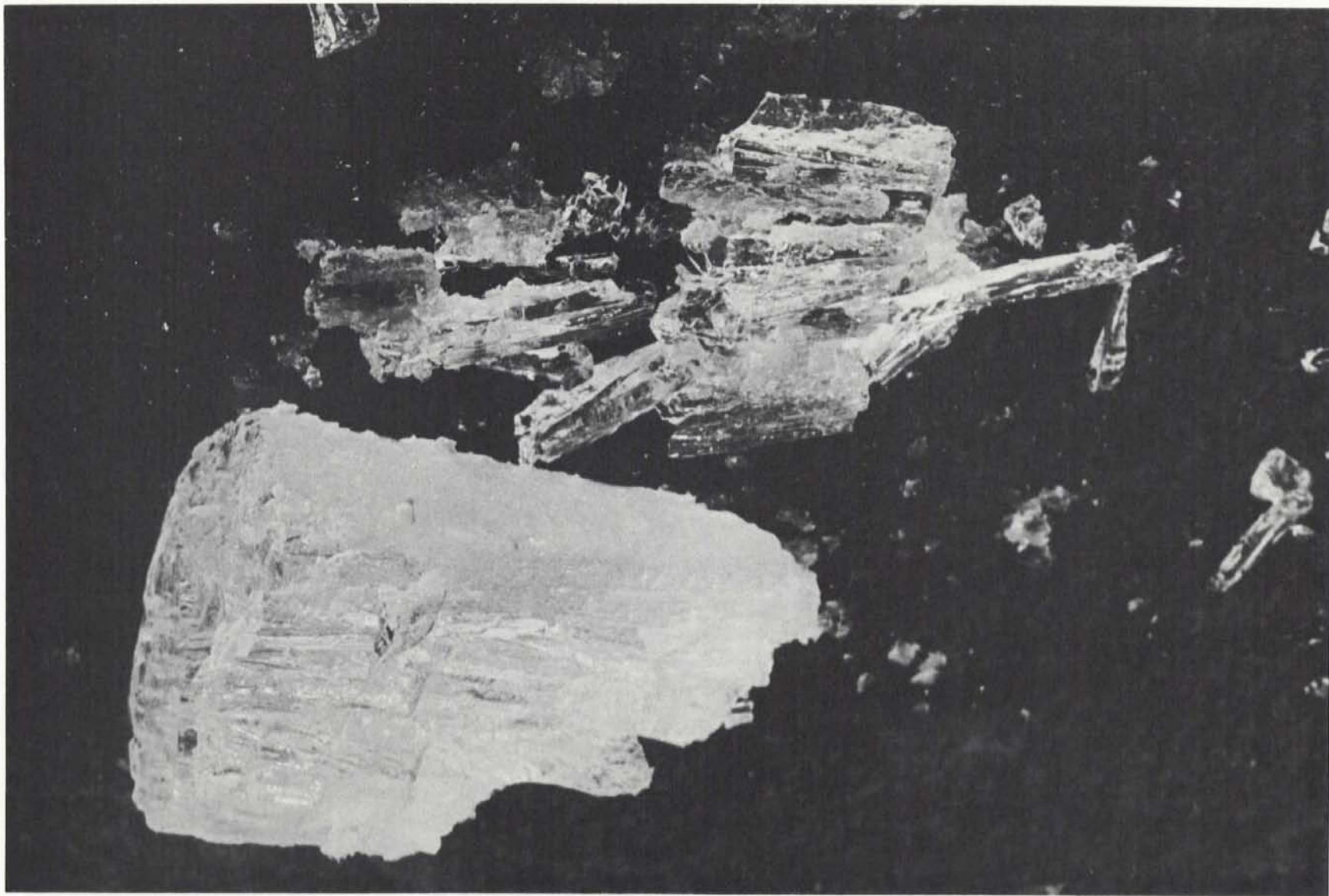


Figure 30. Computer Plot, Air Cushion Vehicle



*Figure 31. Ice Core from DOE Site, Button Bay Area*

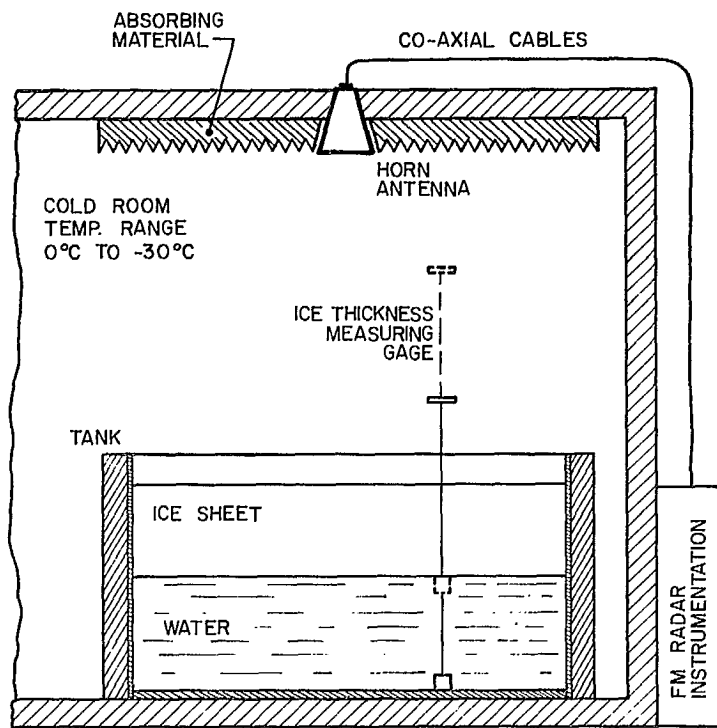


Figure 32. Equipment Installation DOE Laboratory

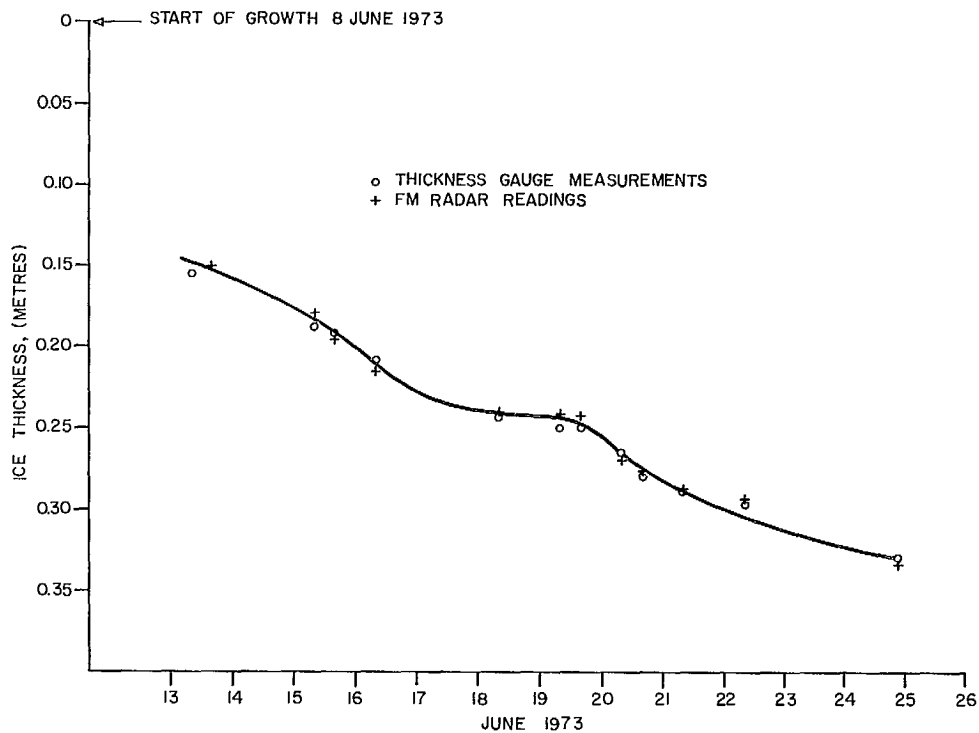


Figure 33. Radar Measurements Versus Ice Gauge Measurements

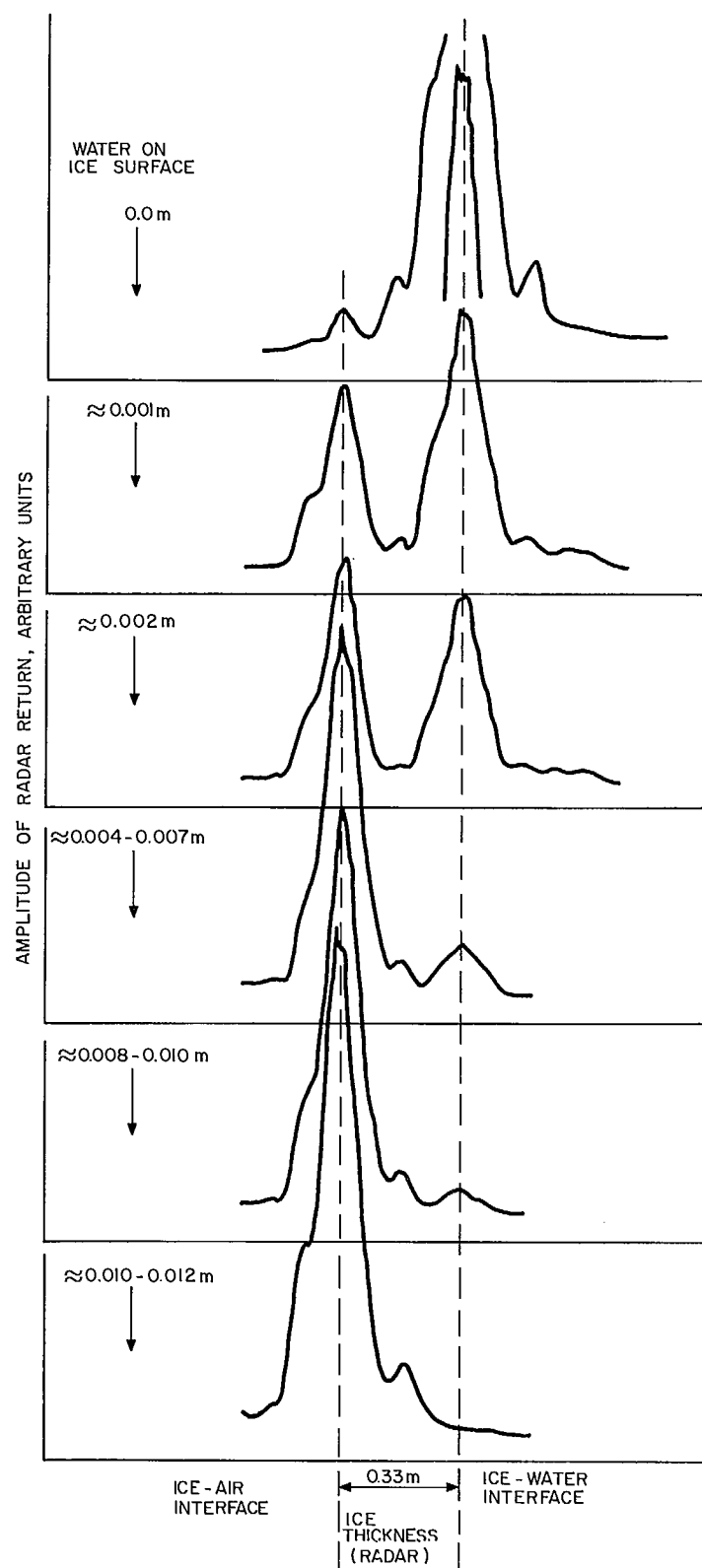


Figure 34. Test Results With Water on Ice Surface

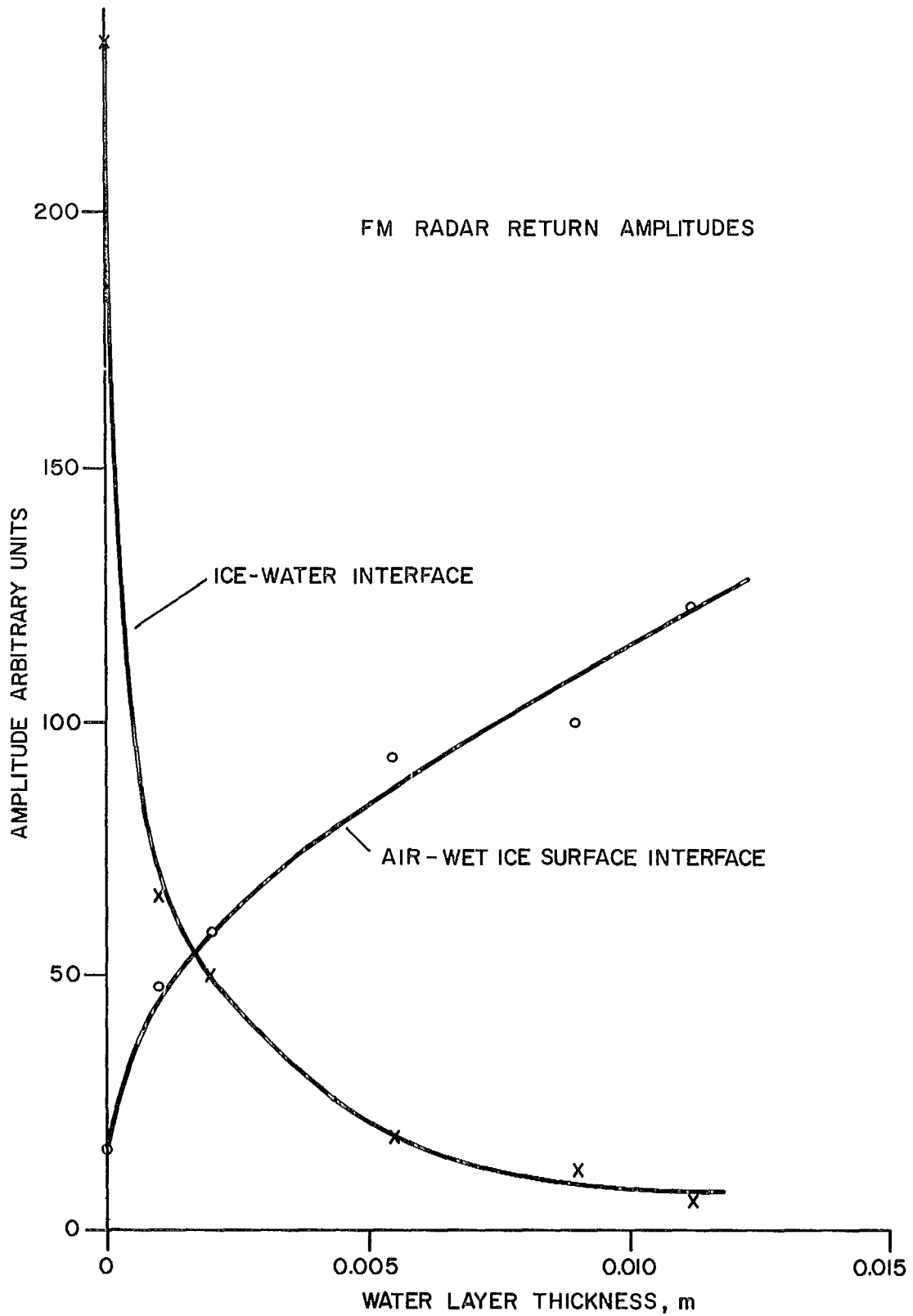


Figure 35. Variation in the Amplitude of the Signal Return From the Water-Ice Interface as a Function of Ice Surface Wetness



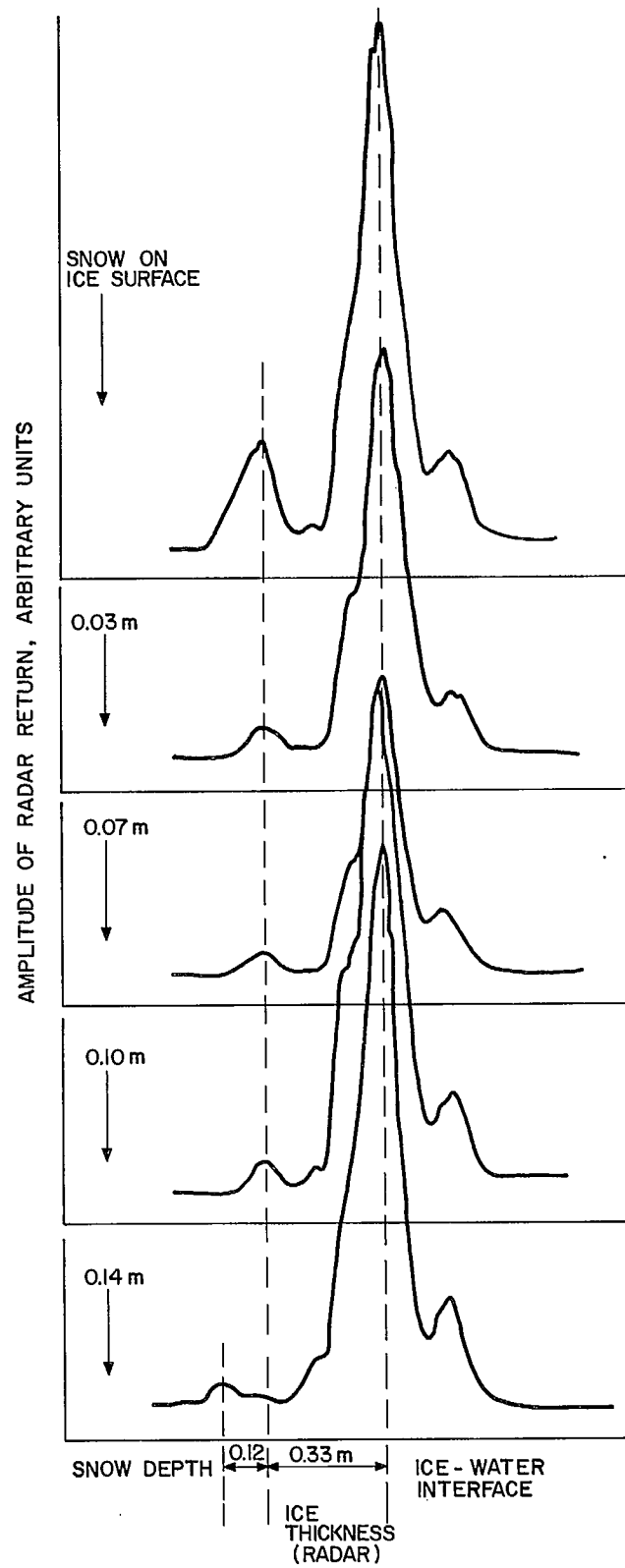


Figure 36. Test Results with Snow on Ice Surface

## CRC DOCUMENT CONTROL DATA

1. ORIGINATOR: Department of Communications/Communications Research Centre

2. DOCUMENT NO: CRC Technical Note No. 673

3. DOCUMENT DATE: October 1975

4. DOCUMENT TITLE: Experiments with a Mobile X-Band FM Radar in Measuring the Thickness of Fresh-Water Ice

5. AUTHOR(s): G.O. Venier, F.R. Cross and R.O. Ramseier

6. KEYWORDS: (1) Radar  
 (2) Ice  
 (3) Measurements

7. SUBJECT CATEGORY (FIELD & GROUP: COSATI)

17      Navigation, Communications, Detection, and Countermeasures

17 09   Radar Detection

8. ABSTRACT: The feasibility of using a high resolution FM radar at X-band frequencies, for measuring the thickness of fresh-water ice from a moving platform, was investigated in a series of field measurements during the winter of 1972/73. The radar was first mounted on a sled and towed over the ice by a snowmobile, and secondly, mounted on an air cushion vehicle and flown over the ice surface. The resolution capability of the radar was adequate for measuring a minimum ice thickness of 14 to 15 centimetres. Received signals were recorded on an audio magnetic tape recorder and processed in the laboratory using a digital computer as well as a slow sweep spectrum analyzer. Radar ice thickness measurements were also carried out during the summer months under controlled conditions in a DOE laboratory. The test results indicate that accurate ice thickness measurements can be carried out with a mobile X-band FM radar.

9. CITATION: \_\_\_\_\_

\_\_\_\_\_







Government of Canada    Gouvernement du Canada

12KT.36001-6-4079-40-357315  
Donald F. Runge Limited, Pembroke, Ontario, Canada